Budget of tropospheric ozone during TOPSE from two chemical transport models

L. K. Emmons,[1] P. Hess,[1] A. Klonecki,[1,4] X. Tie,[1] L. Horowitz,[2] J.-F. Lamarque,[1] D. Kinnison,[1] G. Brasseur,[3] E. Atlas,[1] E. Browell,[5] C. Cantrell,[1] F. Eisele,[1] R. L. Mauldin,[1] J. Merrill,[6] B. Ridley,[1] and R. Shetter[1]

Received 17 June 2002; revised 11 December 2002; accepted 27 February 2003; published 26 April 2003.

[1] The tropospheric ozone budget during the Tropospheric Ozone Production about the Spring Equinox (TOPSE) campaign has been studied using two chemical transport models (CTMs): HANK and the Model of Ozone and Related chemical Tracers, version 2 (MOZART-2). The two models have similar chemical schemes but use different meteorological fields, with HANK using MM5 (Pennsylvania State University, National Center for Atmospheric Research Mesoscale Modeling System) and MOZART-2 driven by European Centre for Medium-Range Weather Forecasts (ECMWF) fields. Both models simulate ozone in good agreement with the observations but underestimate NO_x. The models indicate that in the troposphere, averaged over the northern middle and high latitudes, chemical production of ozone drives the increase of ozone seen in the spring. Both ozone gross chemical production and loss increase greatly over the spring months. The in situ production is much larger than the net stratospheric input, and the deposition and horizontal fluxes are relatively small in comparison to chemical destruction. The net production depends sensitively on the concentrations of H_2O, HO_2 and NO, which differ slightly in the two models. Both models underestimate the chemical production calculated in a steady state model using TOPSE measurements, but the chemical loss rates agree well. Measures of the stratospheric influence on tropospheric ozone in relation to in situ ozone production are discussed. Two different estimates of the stratospheric fraction of O_3 in the Northern Hemisphere troposphere indicate it decreases from 30–50% in February to 15–30% in June. A sensitivity study of the effect of a perturbation in the vertical flux on tropospheric ozone indicates the contribution from the stratosphere is approximately 15%. *INDEX TERMS:* 0368 Atmospheric Composition and Structure: Troposphere—constituent transport and chemistry; 0365 Atmospheric Composition and Structure: Troposphere—composition and chemistry; 0322 Atmospheric Composition and Structure: Constituent sources and sinks; *KEYWORDS:* TOPSE, tropospheric ozone, ozone budget, chemical transport model, stratosphere-troposphere exchange

Citation: Emmons, L., et al., Budget of tropospheric ozone during TOPSE from two chemical transport models, *J. Geophys. Res.*, *108*(D8), 8372, doi:10.1029/2002JD002665, 2003.

1. Introduction

[2] The Tropospheric Ozone Production about the Spring Equinox (TOPSE) campaign, organized by the National Center for Atmospheric Research (NCAR) and sponsored by the National Science Foundation (NSF), was conducted 4 February to 23 May 2000. TOPSE consisted of seven missions, each of which included several flights between Colorado and Churchill, Manitoba, and five of which also were extended to Greenland with sampling over Alert. These missions allowed detailed sampling of the composition of the troposphere in the northern middle and high latitudes from winter through spring. An overview of the campaign is given by *Atlas et al.* [2003].

[3] A key question addressed by TOPSE is the origin of the Northern Hemisphere ozone spring maximum that has been observed in ozonesondes [e.g., *Oltmans and Levy*, 1994], as well as surface measurements [e.g., *Penkett and Brice*, 1986; *Simmonds et al.*, 1997]. Some analyses find that the stratospheric contribution to tropospheric ozone peaks in spring [e.g., *Wang et al.*, 1998], implying that stratospheric flux is the cause of the ozone maximum;

[1]Atmospheric Chemistry Division, National Center for Atmospheric Research, Boulder, Colorado, USA.
[2]Geophysical Fluid Dynamics Laboratory, National Oceanic and Atmospheric Administration, Princeton, New Jersey, USA.
[3]Max Planck Institute for Meteorology, Hamburg, Germany.
[4]Now at NOVELTIS, Ramonville-Saint-Agne, France.
[5]Atmospheric Sciences, NASA Langley Research Center, Hampton, Virginia, USA.
[6]Graduate School of Oceanography, Center for Atmospheric Chemistry Studies, University of Rhode Island, Narragansett, Rhode Island, USA.

0148-0227/03/2002JD002665$09.00

however, other studies propose that chemical production drives the ozone increase [e.g., *Penkett and Brice*, 1986]. Other modeling studies have indicated that the increase in ozone during spring is due to comparable contributions of net chemical production and transport [*Yienger et al.*, 1999]. All of these previous studies had limited observations with which to evaluate their conclusions. The measurements from TOPSE provide information on the key ozone precursors, as well as chemical tracers, which allow us to evaluate model results and constrain our conclusions.

[4] This paper presents an investigation of the ozone budget during TOPSE using two NCAR chemical transport models (CTMs), MOZART-2 (Model of Ozone and Related chemical Tracers, version 2, which is global), and HANK (regional). First, a brief description of the models is given, followed by evaluation of the model results using the various observations of ozone and other species available during this period (section 3). In section 4 the seasonal variation of ozone is presented, and in section 5 the contributions to the ozone budget during TOPSE, determined from the MOZART and HANK results, are presented. Further discussion is given in section 6, and a summary of the conclusions is in section 7.

2. Model Descriptions

[5] The two CTMs used in this study, MOZART-2 and HANK, have similar chemical mechanisms, with detailed O_3 -NO_x -NMHC chemistry, and horizontal resolution, but were driven with different meteorological fields and have different spatial coverage and vertical resolution. Both MOZART and HANK are NCAR community models (further information is available at http://www.acd.ucar.edu/). The use of two CTMs allows greater confidence in our results, as well as providing a means to estimate the uncertainty in such model analyses. Table 1 summarizes the features and differences of the two models, which are briefly elaborated on in the following sections.

2.1. MOZART

[6] A complete description and evaluation of the standard version of MOZART-2, and its improvements over MOZART-1 [*Brasseur et al.*, 1998; *Hauglustaine et al.*, 1998] is given by L. W. Horowitz et al. (A global simulation of tropospheric ozone and related tracers: Description and evaluation of MOZART, version 2, submitted to *Journal of Geophysical Research*, 2002, hereinafter referred to Horowitz et al., submitted manuscript, 2002). MOZART-2 includes a significantly updated chemical scheme, and improved stratospheric constraints and emissions, over MOZART-1. The meteorological fields used to drive MOZART can have a significant impact on the simulated chemical distributions. For the TOPSE campaign, MOZART-2 was driven with meteorological parameters from the European Centre for Medium-Range Weather Forecasts (ECMWF) for 15 January to 3 July 2000 [*European Centre for Medium-Range Weather Forecasts* (*ECMWF*), 1995]. Comparisons of a preliminary version of these MOZART results with observations led to improvements in two aspects of MOZART: the dry deposition scheme and heterogeneous removal of NO_x ($NO + NO_2$). Initially, the simulated ozone mixing ratios in MOZART were much less than observed values in the lower troposphere at high latitudes, suggesting that the dry deposition of O_3 in the Arctic was too large (although already small). The off-line deposition velocities were improved by calculating new deposition fields with meteorological fields and snow cover from NCEP analyses for 1990–1999 using a resistance-in-series scheme [*Wesely*, 1989], which is used online in HANK. Monthly mean values of these deposition velocities were then used in the current simulation (and are now included in the standard version of MOZART-2). The initial model calculations of NO_x were found to significantly underestimate the TOPSE observations. The NO_x abundance is improved when the reaction probability for N_2O_5 is reduced to $\gamma = 0.04$ (see *Tie et al.* [2003] and section 3).

2.2. HANK

[7] The HANK model is described in detail by *Hess et al.* [2000], with changes described by *Klonecki et al.* [2003], and are briefly summarized here. The parameterization of wet removal has been expanded to include the removal of species frozen in ice and the removal of nitric acid that deposits on the surface of ice. The reaction accounting for the heterogeneous removal of N_2O_5 on the surface of aerosols, and a lightning source of NO_x, were added. Ozone in the stratosphere was relaxed to values determined by climatological ozone-potential vorticity correlations with a relaxation time of 5 days. HANK uses the meteorological output fields generated by the Penn State University/National Center for Atmospheric Research (PSU/NCAR) Mesoscale Modeling System (MM5) mesoscale model [*Grell et al.*, 1993] for its temperature, water vapor, pressure, convective mass fluxes and parameters governing diffusive transport and wind fields. The MM5 uses boundary conditions from the NCEP reanalysis and is nudged toward the reanalysis data set. The time- and location-dependent chemical boundary conditions for HANK are derived from a previous global simulation of MOZART.

2.3. Model Differences

[8] Although many aspects of the HANK and MOZART models are similar, there are important differences, as outlined in Table 1. The meteorology, temperature and water vapor as input from ECMWF and MM5 are different, although representing the same time period. Thus the transport fields, including the boundary layer parameterizations and convective mass fluxes, clouds and precipitation are not identical. For the calculations of photolysis rates, HANK uses the observed O_3 columns from TOMS, while MOZART uses the model-calculated ozone field, which is relaxed to climatological values in the stratosphere. Since there was significant Arctic stratospheric ozone depletion in the winter-spring of 2000 [*Richard et al.*, 2001; *Sinnhuber et al.*, 2000], MOZART overestimates the ozone column in February–April over parts of the Arctic by up to 10%. The large-scale and convective rainout parameterizations differ considerably between the two models, and MOZART does not treat washout on snow and ice differently than rain. The off-line dry deposition scheme used in MOZART is derived from that in HANK, but uses climatological dry deposition velocities, whereas HANK calculates deposition online. The chemical mechanisms are both derived from that given by

Table 1. Comparison of the MOZART and HANK Models

	MOZART	HANK
Domain	global	north of ≈20°N[a]
Meteorology	ECMWF	MM5 [b]
Horizontal resolution	2° lon × 1.9° lat	243 km, polar projection
Layers in vertical	60 layers to 0.1 hPa	38 layers to 100 hPa
Layers below 850 hPa	11	8
In-cloud washout	*Giorgi and Chameides* [1985]	*Giorgi and Chameides* [1985]
Below-cloud washout	*Brasseur et al.* [1998]	*Giorgi and Chameides* [1985][c]
Ice scavenging	...	*Klonecki et al.* [2003][d]
Convective washout	*Brasseur et al.* [1998]	*Hess* [2001]
Lightning[e]	*Price et al.* [1997]	*Price and Rind* [1992]
Dry deposition	*Wesely* [1989][f]	*Wesely* [1989]
Photolysis lookup table	TUV, L. W. Horowitz et al. (manuscript in preparation, 2003)	*Hess et al.* [2000]
O_3 Column (for photolysis)	model-simulated[g]	TOMS O_3 for 2000
Stratospheric O_3	based on climatological O_3[g]	based on PV correlation[h]
Other stratospheric species	from STARS model[i]	based on O_3 correlation[j]
Chemistry[k]	updated *Müller and Brasseur* [1995]	updated *Müller and Brasseur* [1995]
Emissions[l]	derived from EDGAR *Olivier et al.* [1996]	derived from EDGAR *Olivier et al.* [1996]
Aerosol distribution	climatological, *Tie et al.* [2001]	Climatological, *Barth et al.* [2000]
Reaction probability	0.04	temperature, RH-dependent[m]

[a]HANK southern boundary does not coincide with a latitude line.
[b]Initial and boundary conditions from NCEP are used, and MM5 is nudged to the NCEP analysis.
[c]Washout rate is ten times higher in-cloud than below cloud *Klonecki et al.* [2003].
[d]Deposition of HNO_3 on ice surfaces following *Abbatt* [1997]. See *Klonecki et al.* [2003].
[e]Vertical distribution in each case based on *Pickering et al.* [1998].
[f]Based on climatological NCEP meteorological fields.
[g]Stratospheric O_3 is relaxed to monthly mean climatology based on ozonesondes [*Logan*, 1999] and HALOE [*Randel et al.*, 1998] with a relaxation time of 10 days.
[h]Relaxed to monthly mean climatological correlation of O_3 and potential vorticity derived from ozonesondes with a relaxation time of 5 days [see *Klonecki et al.*, 2003].
[i]Long-lived species only [*Brasseur et al.*, 1997].
[j]HNO_3 only; other species specified from a MOZART simulation.
[k]Chemistry schemes differ in oxidation mechanism for higher hydrocarbons [see *Klonecki et al.*, 2003; L. W. Horowitz et al., manuscript in preparation, 2003].
[l]See Horowitz et al. (manuscript in preparation, 2003).
[m]Based on temperature and relative humidity dependence given by *Hallquist et al.* [2000], but reduced substantially in magnitude [see *Klonecki et al.*, 2003].

Müller and Brasseur [1995]. The mechanisms have recently been compared and differ in some details of the oxidation mechanism of the higher hydrocarbons. The emissions are also similar, both derived from the EDGAR database [*Olivier et al.*, 1996] and *Müller* [1992] and are climatological, not specifically for the period of simulation. Table 2 summarizes the emissions of a few species north of 30 N used in HANK and MOZART. The emissions used in HANK were from the inventory used in an intermediate version of MOZART, while the MOZART emissions shown here were further refined on the basis of evaluation of interim model runs (cf. Horowitz et al., submitted manuscript, 2002). The difference between the two emission inventories used is an indication of their uncertainty. For example, differences in CO emissions are accounted for by differences in emission factors for biomass burning and soil emissions.

[9] As shown by *Tie et al.* [2003] the model results are sensitive to the hydrolysis of N_2O_5 on sulfate aerosols. The sulfate aerosol concentration also differs between the two models, with the MOZART aerosol distribution taken from a MOZART-1 simulation (see above), while the HANK distribution is from *Barth et al.* [2000] and *Rasch et al.* [2000]. In MOZART the sulfate surface area was calculated at a given aerosol radius (0.15 μm) and it grows with relative humidity, which is calculated online. In HANK the aerosol surface area also grows with relative humidity assuming a lognormal distribution and the method given by [*Kiehl et al.*, 2000]. Efflorescence was assumed to occur at 35% relative humidity regardless of temperature. A temperature dependence was assigned to the reaction probability following the results of *Hallquist et al.* [2000], although the rates were significantly lowered to increase NO_x to better agree with observations (see *Klonecki et al.* [2003] for more details).

3. Evaluation of MOZART and HANK With TOPSE Data

[10] The TOPSE campaign has provided an extremely valuable data set for model evaluation as there were previously only limited observations available in this region during winter and spring. Since MOZART and HANK were driven with meteorological fields for the period of TOPSE,

Table 2. Surface Emissions North of 30 N for HANK and MOZART (Tg/year)

	MOZART		HANK	
Species	Feb	May	Feb	May
NO	44.0	45.0	41.3	43.1
CO	430.6	474.9	349.5	416.7
C_2H_6	4.4	4.1	7.1	6.4
C_3H_8	4.7	4.4	8.8	8.0

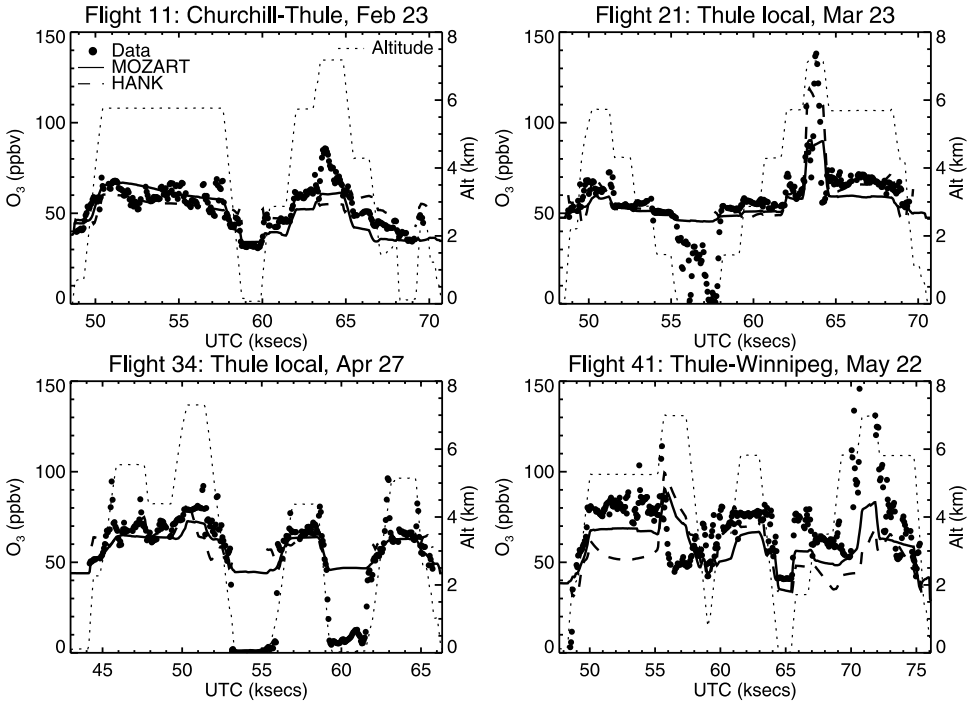

Figure 1. In situ ozone observations along the flight track for 4 flights with MOZART (from 24-hour averages) and HANK (from 6-hour averages) results interpolated to the flight path (1-min averages). The flight altitude (dashed line) is plotted against the right axis.

it is appropriate to make point-by-point comparisons of the model results to the observations. To accomplish this, the model results were interpolated from the model grid points to the flight track. Comparison with parameters most directly affecting ozone chemistry are shown here. Additional comparisons of MOZART against NO_x measurements are given by *Tie et al.* [2003], CO measurements of *Lamarque and Hess* [2003] and HANK is compared against hydrocarbon measurements of *Klonecki et al.* [2003]. In general, both models reproduce the CO and hydrocarbon data. However, MOZART overestimates CO in late winter, probably due to the emissions being too large, and HANK underestimates CO in late spring because of too large OH concentrations. NO_x mixing ratios in both models are lower than the observations, as shown below. Details of the measurements are given in other papers [*Ridley et al.*, 2003; *Cantrell et al.*, 2003; *Mauldin et al.*, 2003; *Browell et al.*, 2003; *Shetter and Müller*, 1999; *Shetter et al.*, 2002]. All data shown here are from the 1-min merged data set, and model results along the flight track are interpolated from instantaneous values at 3-hour intervals to this time base.

[11] Figure 1 shows the comparison of in situ O_3 data with MOZART and HANK for four flights that are representative of the latitude and seasonal conditions sampled. In general, both models reproduce the observations well. Extremely low values of O_3 were seen in the boundary layer in the Arctic (e.g., flights 21 and 34), possibly due to destruction by bromine [*Ridley et al.*, 2003]. MOZART and HANK do not include halogen chemistry so these depletion events were not simulated in either model. Most of the variation in ozone with time is correlated with altitude. Occasionally, values of 100 ppbv or higher were observed along the highest flight legs, indicative of stratospheric influence. The models are able to reproduce some of these features (e.g., flight 21), though not all (e.g., flight 41), probably a result of the coarse horizontal resolution of the model results, and inaccuracies in the meteorological fields.

[12] Several parameters were measured during TOPSE that are critical to the ozone budget, including the photolysis frequency of $O_3 \rightarrow O(^1D)$ ($J(O_3)$), and concentrations of NO_x, H_2O, OH and $HO_2 + RO_2$ ($RO_2 = CH_3O_2$ + other peroxy radicals). To more easily see the discrepancies between the models and observations, scatterplots of the correlation between the data and model results along the flight tracks for 4 altitude bins (including all latitudes and missions) are shown in Figure 2. The results of the correlations over all altitudes are summarized in Table 3. The correlation coefficients (R) are a rough indication of the amount of scatter in the correlations. The low values of R are also a result of meteorological noise and the lack of large gradients in space or time. The correlations for data binned by latitude for north and south of 60°N are similar to the results shown for all-latitudes.

[13] Both models underestimate O_3 on average, except in the high-altitude bin. NO_x is underestimated on average, with greater error at higher altitudes. It is not clear how to resolve the discrepancies between the modeled and measured NO_x. Of the model processes included in the NO_x budget, the most uncertain is probably the heterogeneous removal of N_2O_5 on aerosols. Both the aerosol distribution and the reaction probability are not well known. While *Tie et al.* [2003] demonstrate that the overall budget of NO_x is sensitive to this removal, the sensitivity is small. Varying the heterogeneous removal of N_2O_5 within reasonable ranges is

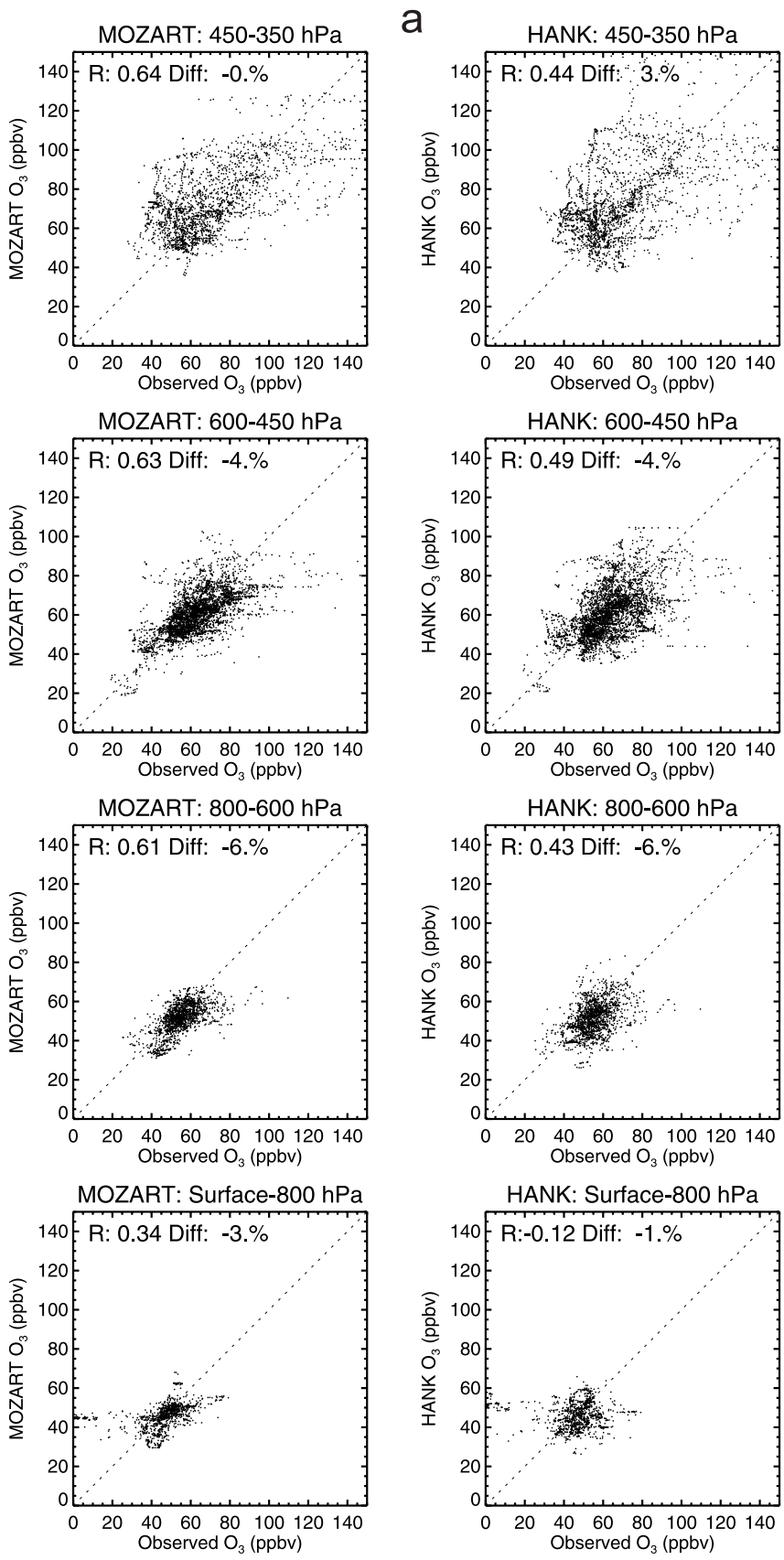

Figure 2. Correlation plots of observations with model results along the flight tracks MOZART (left panels) and HANK (right panels), for four altitude bins (approximately 2 km each): (a) O_3, (b) NO_x, (c) $J(O_3)$, (d) H_2O, (e) $HO_2 + RO_2$, (f) OH. The correlation coefficients and median of the differences are shown for each bin.

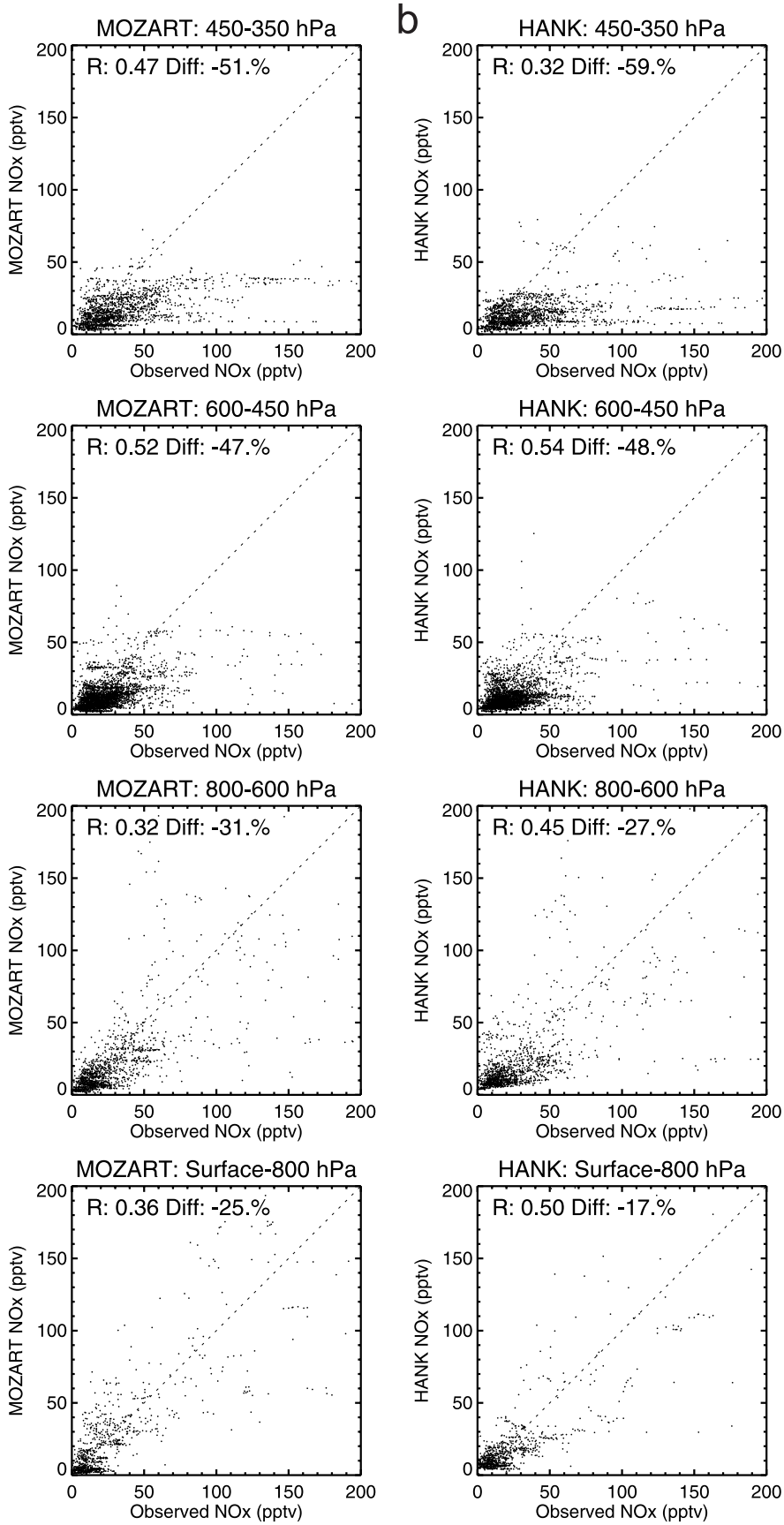

Figure 2. (continued)

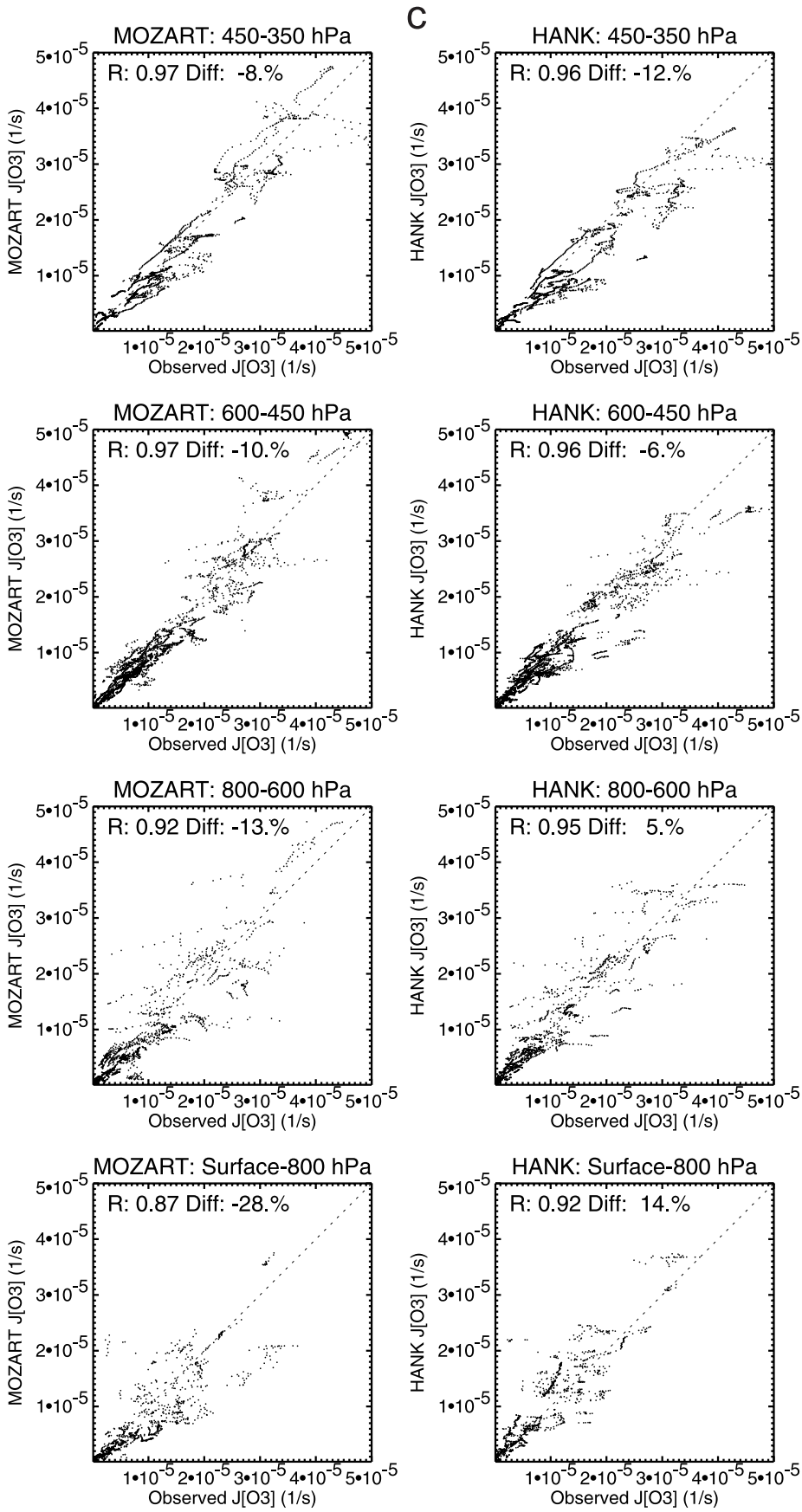

Figure 2. (continued)

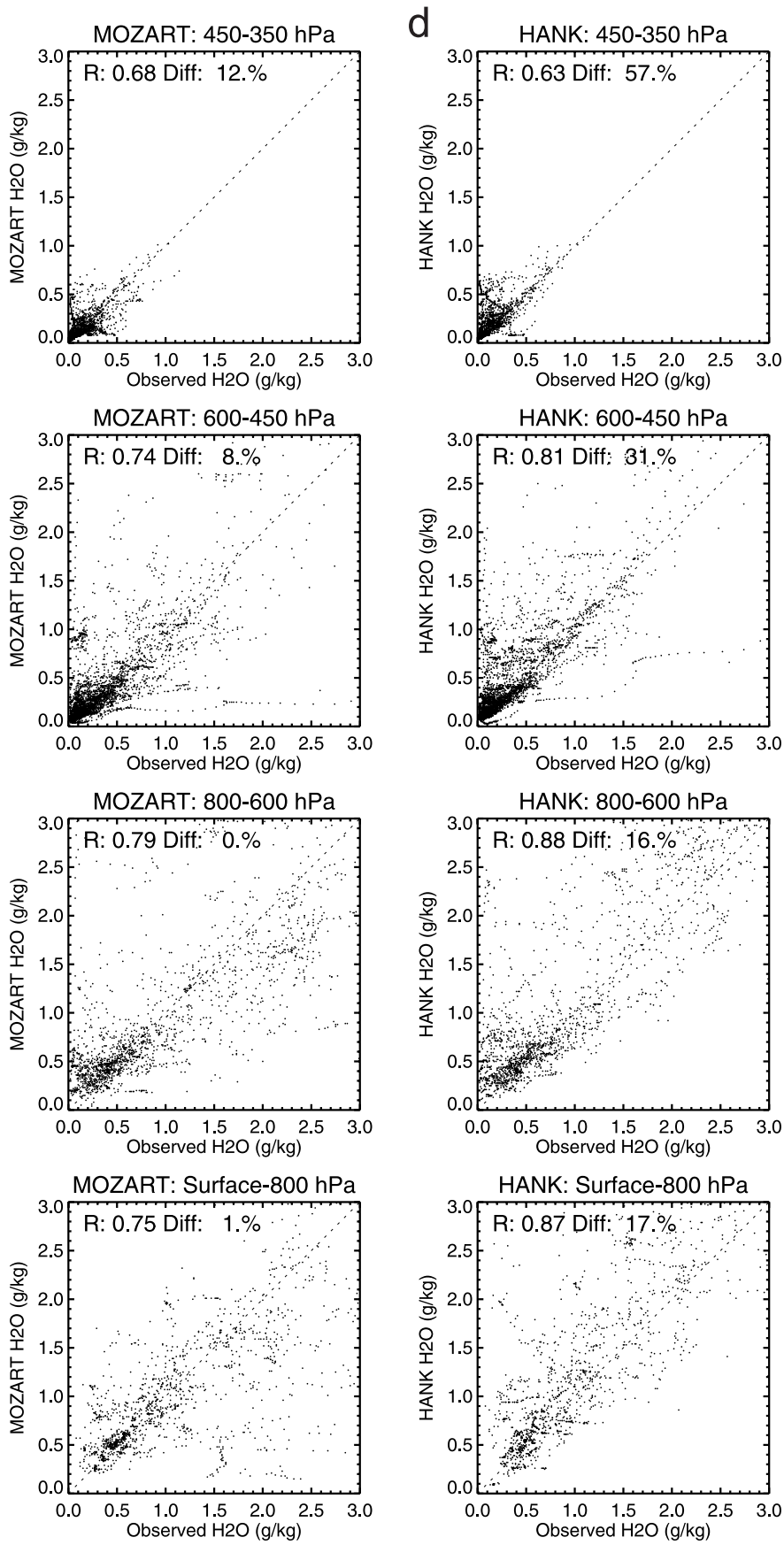

Figure 2. (continued)

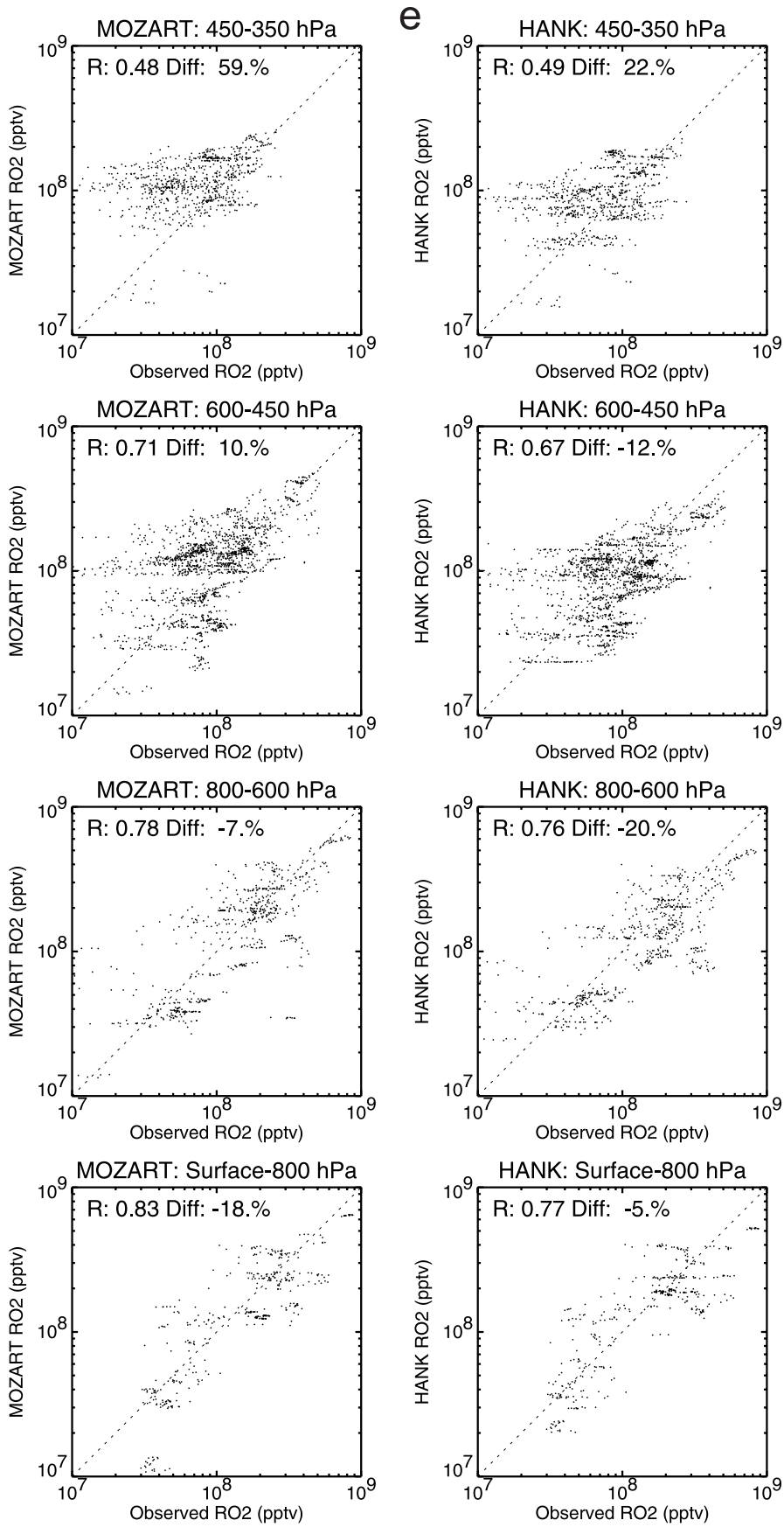

Figure 2. (continued)

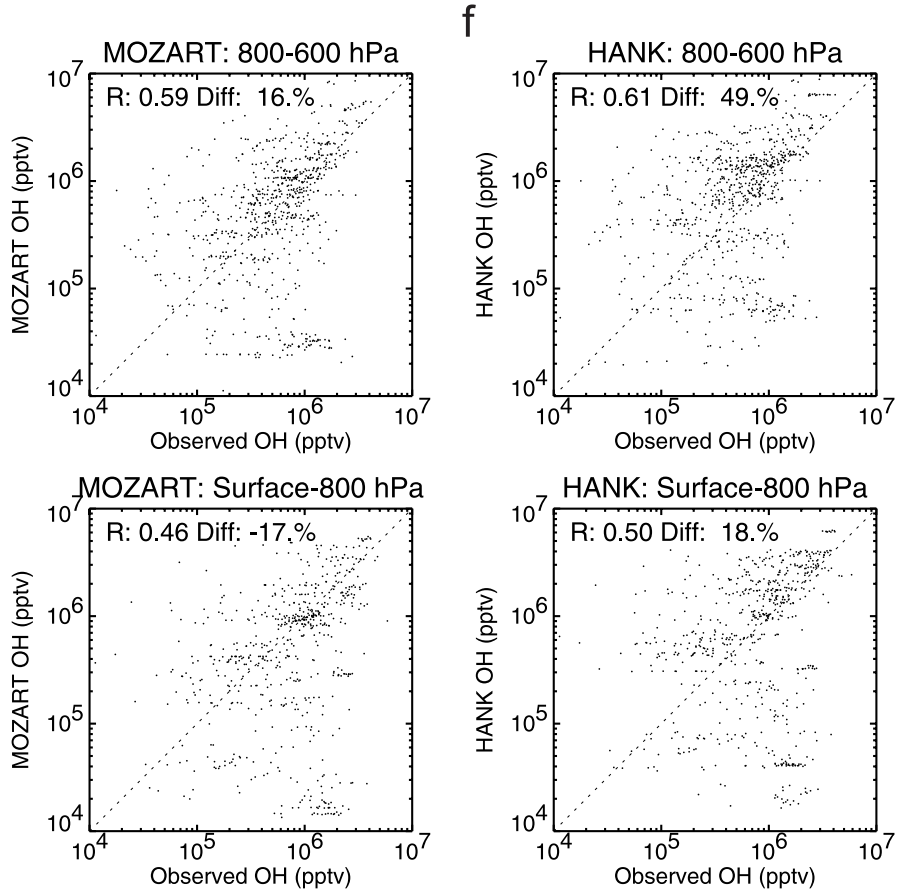

Figure 2. (continued)

not sufficient to obtain the measured NO_x concentrations. This is because the reaction of NO_2 and O_3 is usually the rate limiting step. It is not clear what process is responsible for the underestimate of simulated NO_x. This error in NO_x implies the model ozone production rates will be underestimated, and is consistent with the underestimate of O_3.

[14] MOZART significantly underestimates the photolysis frequency of O_3, with greater error at lower altitudes. In both models, the relative errors at solar zenith angles greater than 80° are significantly worse due to the greater difficulty of determining airmass factors in the models at high zenith angles, and errors due to interpolating to the time and location of the observations across sunrise or sunset. The calculated photolysis rates in both models are corrected for the effect of clouds, however, some of the model error is certainly attributable to errors in the assumed cloud cover. MOZART shows good agreement with the observations of H_2O, while HANK is distinctly higher. The water vapor in HANK is imported from the MM5 simulation, while in MOZART it comes from the ECMWF analysis. There is a large amount of scatter in the RO_2 and OH correlations, indicative of the difficulty of the measurement, as well as the difficulty of modeling these short-lived radicals (OH is only available below 3 km [see *Mauldin et al.*, 2003]). On average, the agreement is good, however, HANK overestimates OH, which is at least partly attributable to the overestimates of H_2O and $J(O_3)$ in the lower troposphere.

[15] During the TOPSE campaign ozonesondes were launched in coordination with the aircraft flights, in particular at Boulder and Churchill. Ozonesondes are also launched regularly at a number of other sites throughout Canada (archived at the World Ozone and Ultraviolet Data Centre). The sonde data provide a time series of ozone throughout the troposphere and lower stratosphere, which is quite valuable for model evaluation. Figure 3 shows the comparison of MOZART and HANK with ozonesonde data at Churchill (Figures 3a and 3b), Boulder (3c) and Alert (3d), with both observations and model results binned by the indicated altitude ranges. The model results plotted are instantaneous values every 3 hours. The correlation coefficients and median difference in each altitude bin between

Table 3. Correlation Coefficient (R) and Median of the Differences Between the MOZART or HANK Model Results and the Observations (for the Entire Data Set, Except as Indicated)

	MOZART		HANK	
Species	R	Difference, %	R	Difference, %
O_3	0.70	−4	0.56	−3
NO_x	0.30	−43	0.43	−44
$J(O_3)$ (SZA < 80°)	0.95	−11	0.94	−5
$HO_2 + RO_2$	0.77	10	0.76	−6
OH	0.50	−1	0.53	33
H_2O	0.84	0	0.91	21

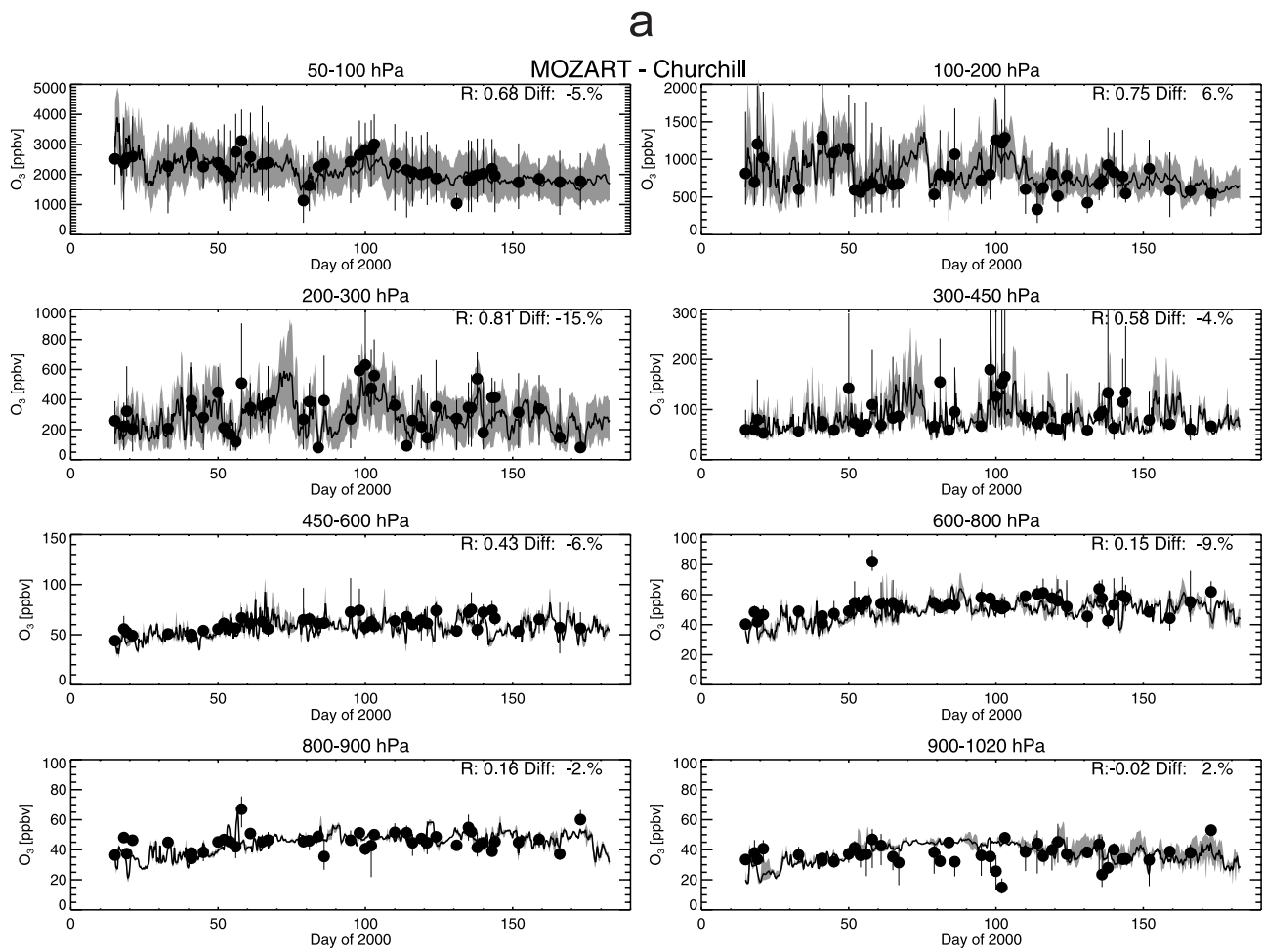

Figure 3. Mean values of ozonesondes (circles) at Churchill averaged over 8 altitude bins, with model results (solid line) from (a) MOZART and (b) HANK. MOZART and HANK for 4 lower stratosphere to midtroposphere altitude bins at (c) Boulder and (d) Alert. The model results are instantaneous values every 3 hours. The error bars and shading represent the ranges within each altitude range for the sondes and models, respectively. The correlation coefficients and median of the differences are shown for each altitude bin.

each model (interpolated to the times of the sonde data) and the sondes are shown on the plots. Very good agreement is seen for both models at Churchill, from the surface into the lower stratosphere. Since upper tropospheric ozone is largely influenced by the stratospheric flux [*Lamarque et al.*, 1999], these comparisons suggest the cross-tropopause flux in the models is reasonably accurate. Good agreement in the boundary layer also indicates the surface deposition is reasonable in the models. Both models capture the ozone increase until approximately day 100 below 600 hPa at Churchill. The HANK results at low altitudes hint at an ozone decrease after day 120 which is not shown in the data or MOZART. Similarly good agreement is generally seen for Boulder and Alert, for which just the upper troposphere and lower stratosphere results are shown (Figures 3c and 3d). Note that, in general, the level of agreement is similar for the two models at all three sites, even though the meteorology and the stratospheric ozone is handled quite differently in the two models. Both models capture the day-to-day variability seen in the sondes, as well as the variations in height. Much of the variability is probably due to meteorology and dynamics, such as tropopause folds and synoptic systems, and this is determined by the meteorology driving the models.

4. Ozone Seasonal Evolution

[16] To study the evolution of tropospheric ozone through spring, averages over all latitudes and altitudes for each mission were made of the TOPSE in situ and DIAL O_3 measurements, and are shown in Figure 4. Since the DIAL data include measurements above and below the flight track (but not at it) these data represent a different sampling of the region (only data below 8 km are included here). Both the in situ and DIAL data show a significant increase through the spring, including into May. The in situ data appears to be representative of the DIAL O_3 measurements until the last campaign, when the in situ measurements are notably higher. The HANK and MOZART results along the flight tracks (i.e., interpolated as described in section 3) both suggest an ozone increase through April, as do the data, and both underestimate the measured ozone along the flight

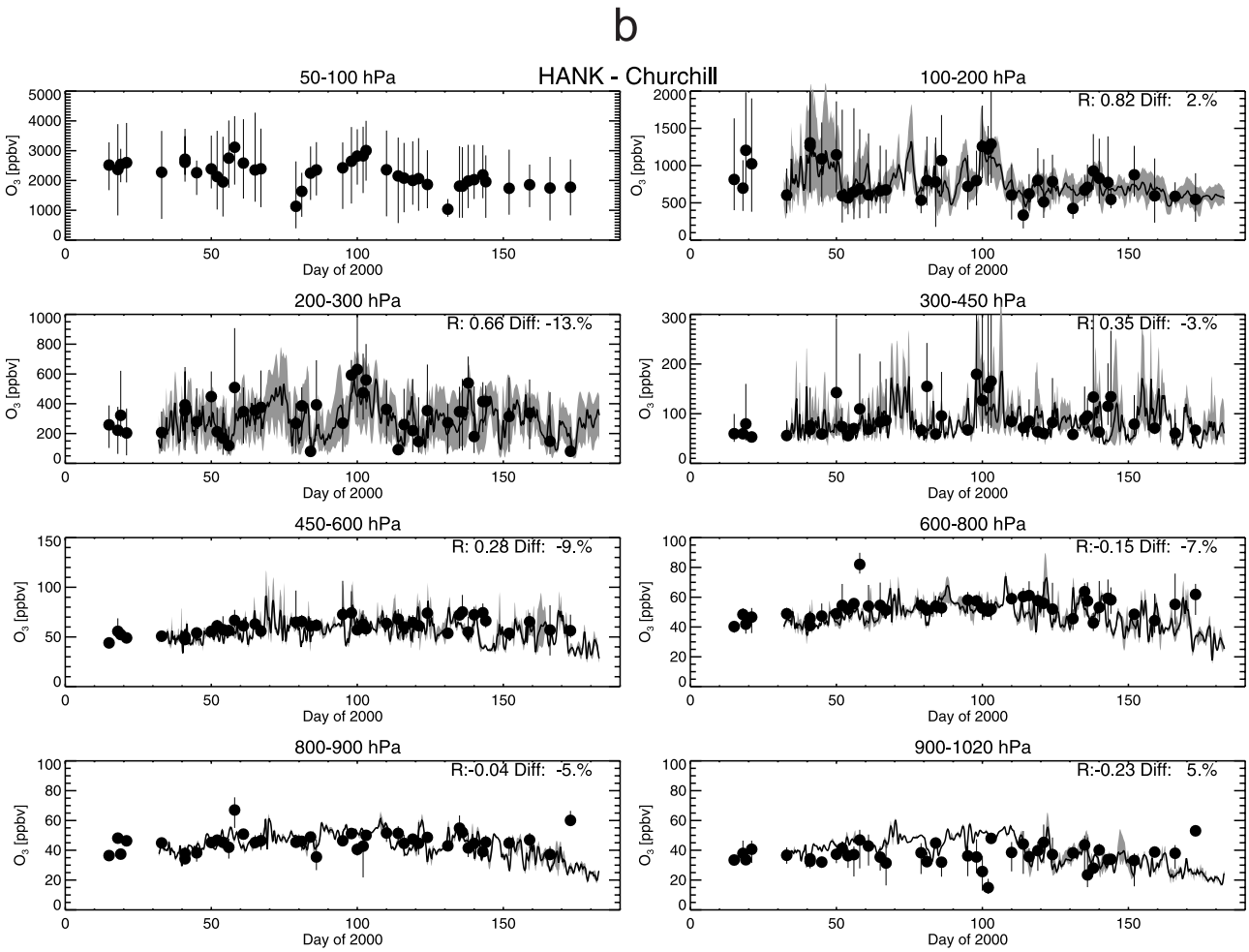

Figure 3. (continued)

track during the last mission in mid-May. Further analysis of these model differences is discussed below.

[17] For comparison, the MOZART and HANK results have been averaged for each month over the entire North American troposphere in the TOPSE region (40°N–85°N, 235°E–300°E, surface to 350 hPa). Comparison of the North American average to the flight track averages gives an indication of how representative the TOPSE data are of the whole region. For March through May, the monthly continental-scale means are similar to the flight track results (averages within 5 ppbv) indicating the TOPSE observations were representative of the North America region. For February, however, the MOZART monthly mean is significantly less, which indicates the TOPSE flight track encountered some conditions that were possibly not typical of the larger region. MOZART and HANK both show maximum O_3 in April for North America and along the flight tracks, whereas the observations increase through May.

5. Ozone Budget From MOZART and HANK

[18] The various contributions to the ozone budget have been analyzed from the MOZART and HANK simulations in order to understand the cause of the increase of ozone through the spring. The budget of the northern middle and high latitudes is analyzed for a zonal volume encompassing 30°–90°N and pressures greater than 350 hPa. Since the lifetime of ozone is long (2 months at midlatitudes and up to 10 months at high latitudes), especially during winter, a hemispheric-scale budget analysis is more appropriate than a study of the TOPSE region. The top of this region is the model level closest to 350 hPa for both models. This altitude was chosen to match the top of the TOPSE measurements, and is close to the tropopause. Although highly variable, *Holton et al.* [1995] shows the climatological mean tropopause height is located between 300 and 400 hPa north of 30°N in winter, and in MOZART it is at approximately 300 hPa in winter.

[19] Figure 5a shows the total ozone mass for the study region on the first day of each month. The two model results are almost identical, showing an increase through April, but HANK drops off more rapidly starting in May (see discussion of ozonesondes above). The shape of the seasonal evolution is consistent with the model results over the TOPSE region shown in Figure 4. Although the aircraft observations do not indicate a decrease in O_3 by mid-May, the ozonesondes, plotted through June in Figure 3, do show such a trend.

[20] The rate of change of ozone can be expressed as:

$$\frac{dO_3}{dt} = V + H + P - (L + D)O_3, \qquad (1)$$

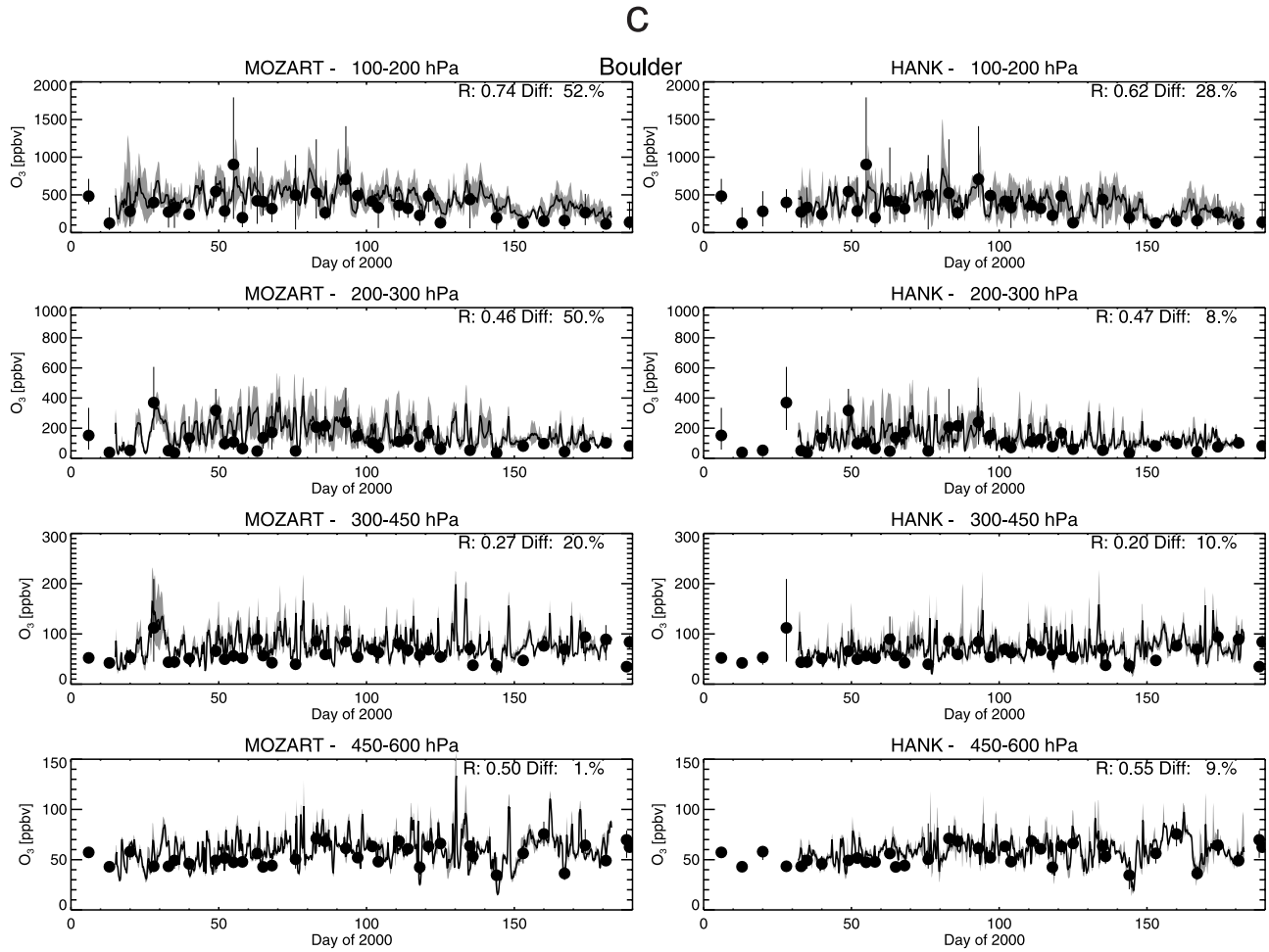

Figure 3. (continued)

where V and H are the vertical and horizontal transport flux respectively, P and L are chemical production and loss rates, and D is the deposition rate. Figure 5b shows each of these components of the ozone budget from MOZART and HANK for the study region: net chemistry ($P - LO_3$), downward vertical flux at 350 hPa (V), northward horizontal flux across 30°N (H), and deposition (DO_3). The vertical flux in HANK is primarily vertical advection, but it also includes vertical diffusion, convection and the rearrangement of ozone mass due to inconsistencies between the wind fields and the surface pressure tendency [cf., *Jöckel et al.*, 2001]. The flux is calculated as a residual of the actual ozone change, the change due to chemistry and the change due to horizontal fluxes. In MOZART, the vertical flux shown is simply the vertical advective flux. MOZART includes a similar rearrangement of ozone mass, but it is small on average.

[21] The vertical flux at 350 hPa increases steadily in both models from 15 Tg/mon in February to 30 Tg/mon for MOZART and 50 Tg/mon for HANK in June. The change due to net chemistry in MOZART increases from 10 Tg/mon in February to 35 Tg/mon in June, while in HANK the net chemical production peaks in March at 10 Tg/mon, dropping to 5 Tg/mon in May and −2 Tg/mon in June (i.e., net destruction). The greater vertical influx of ozone in HANK is compensated for by less net ozone production. The two models show comparable rates of horizontal flux out of the region (i.e., across 30° N) and deposition, which contribute to an increasing loss in ozone through the spring. The horizontal flux is negative, indicating an export of ozone from the middle and high latitudes of the Northern Hemisphere. The increase in the magnitude of the deposition flux (proportional to ozone concentration and deposition velocity) reflects the change in land surface properties, and possibly meteorology, with season. Note that the rate of ozone removal by deposition in HANK in late spring is somewhat less than that in MOZART because the ozone is less.

5.1. Transport Versus Chemistry

[22] As is evident from equation (1), the chemical production and transport terms of the ozone budget are not explicitly dependent on the ozone concentration (to a first approximation), while the chemical loss and deposition terms are. Loss and deposition operate on ozone regardless of whether it is chemically produced in a region or transported into that region. Therefore the net chemical production ($P - LO_3$), reflects the loss of both transported ozone as well as chemically produced ozone. Thus it is not appropriate to compare transported ozone and net chemical production. The chemical production of ozone has been plotted with the vertical and horizontal transport fluxes in Figure 5c, while the chemical destruction and deposition are plotted in Figure 5d. The interpretation of

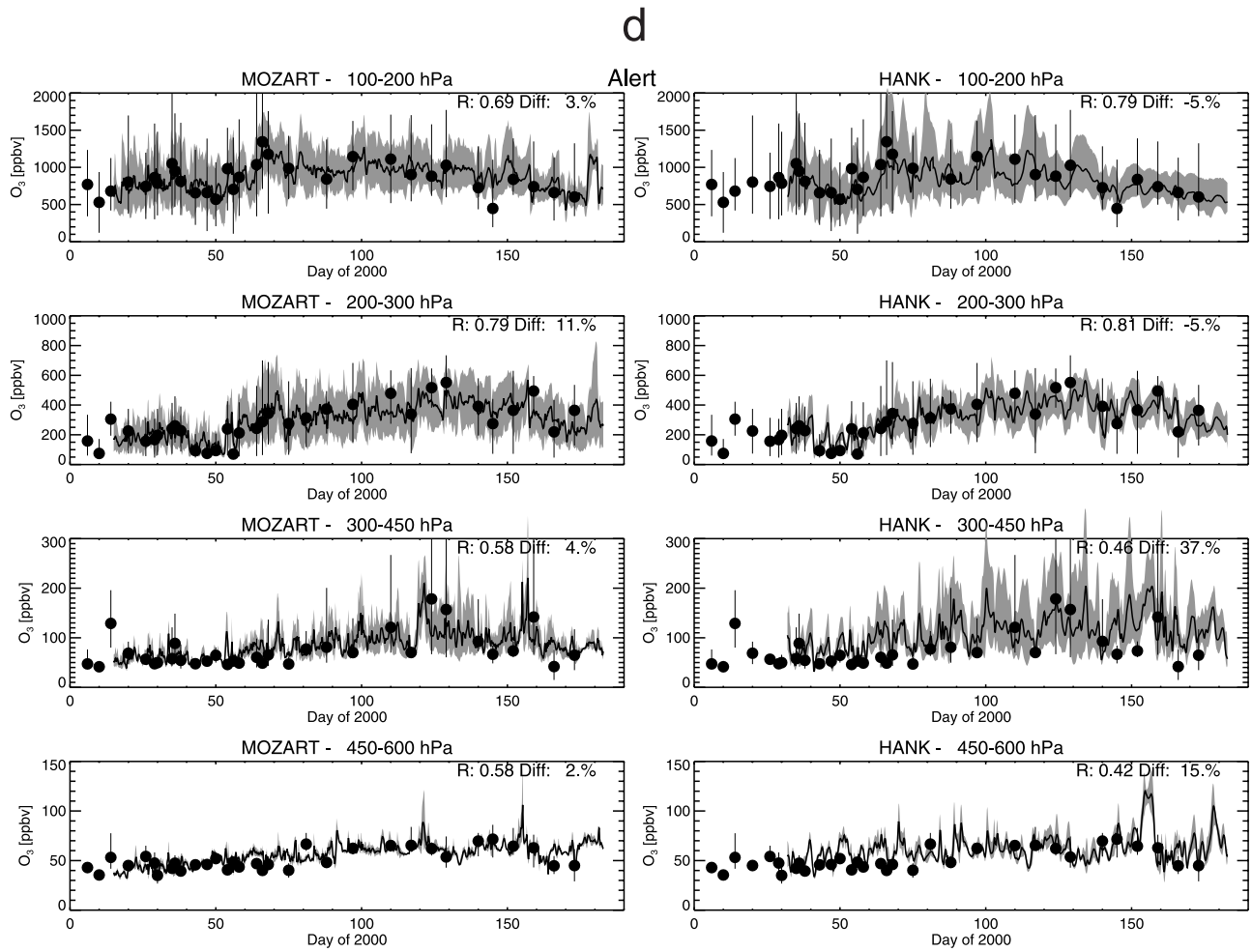

Figure 3. (continued)

net vertical flux is discussed further in section 5.6. The net chemistry rates shown in Figure 5b are the total changes in ozone due to chemistry, whereas the production and loss rates in Figures 5c and 5d are determined from the rate-limiting reactions, with minimal contribution from null cycles. Here we take the rate of O_3 production as the sum of the reactions of HO_2 and RO_2 with NO, and the O_3 destruction rate shown is the sum of the losses due to $HO_2 + O_3$, $OH + O_3$, and $H_2O + O(^1D)$ [e.g., *Brasseur et al.*, 1999]. The difference of the chemical production and loss rates calculated in this way does not exactly equal the net production, however, the differences are small and do not change the conclusions drawn here.

[23] For this Northern Hemisphere region, chemical production of ozone is 2–5 times greater than the net vertical and horizontal transport into the region, increasing steadily through the season. Surface deposition is about half that of the chemical destruction of ozone. Therefore, for both MOZART and HANK, the O_3 chemical production and loss terms are the dominant terms in a calculation of the net sources and sinks.

5.2. O_3 Chemical Production and Loss Terms

[24] The chemical ozone production and loss are almost in balance in both models, with the net production being the difference between two large terms. Therefore changes in these terms may have an important effect on the net production. The main discrepancies in the chemical budgets between HANK and MOZART are that the ozone loss in HANK is slightly higher in February to April, and the ozone production in MOZART is significantly higher after April (e.g., 40 Tg/mon higher than HANK in June). The contributions of each of the most significant reactions to the ozone production and loss rates were calculated off-line from instantaneous values every 3 hours, and are shown in Figure 6. $HO_2 + NO$ is the dominant source of O_3 throughout this period. From Figure 6a it is evident that the greater increase in ozone production in MOZART than in HANK is mainly due to $HO_2 + NO$, which is a result of more HO_2 in MOZART in May and June (not shown). The comparison with aircraft measurements of $HO_2 + RO_2$ also suggests MOZART is biased high with respect to HANK overall (Figure 2e), which may be due to differences in the efficiency of the convective transport in the two models.

[25] Figure 6b shows that $HO_2 + O_3$ and $H_2O + O(^1D)$ are the most important contributions to the total ozone destruction. Each of the terms increases through the spring, but at different rates. 50% of the chemical loss in February is due to $HO_2 + O_3$, but in June $H_2O + O(^1D)$ contributes 50%, while $OH + O_3$ is a constant 15% of the total. $H_2O + O(^1D)$ is the reaction with the highest discrepancy between the two models in the early part of the campaign. Although the

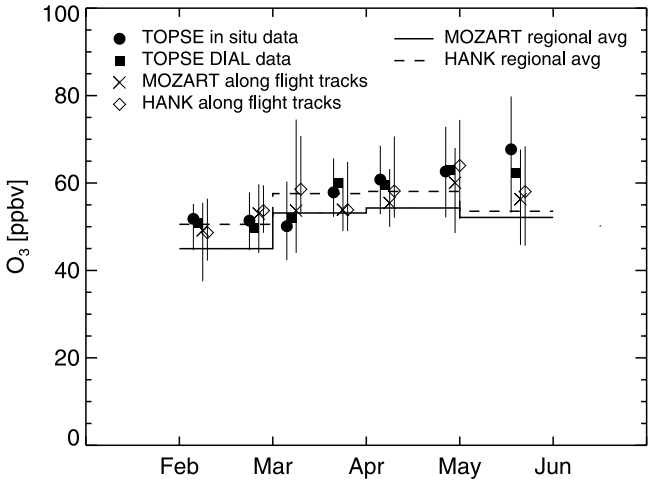

Figure 4. Ozone averaged over North America: in situ data, DIAL data, MOZART and HANK along flight tracks, and monthly means of the models for 40°–85°N, 235°–300°E, surface to 350 hPa. Symbols indicate medians and error bars span central 50% of data. Median of DIAL data below 8 km is shown. Data and model results are slightly offset along x axis at date of each mission.

models differ significantly in their ability to reproduce the observed $J(O_3)$ values (Figure 2c) the total masses of $O(^1D)$ for the two models (not shown) agree quite well. The comparison of the H_2O mass mixing ratio along the flight tracks (Figure 2d) suggests that HANK is biased high with respect to the measurements, while MOZART agrees well on average. The higher water vapor in HANK explains the greater importance of the loss of ozone through $O(^1D)$ and the higher concentrations of OH. This suggests there is a chemical model sensitivity to water vapor distribution, and implies possible sensitivities in estimating the chemistry in climate change scenarios [e.g., *Thompson et al.*, 1990].

5.3. Budget for High Latitudes

[26] Since a significant fraction of the TOPSE flights were between 60°–90°N, and the temperatures and solar radiation are significantly different from lower latitudes, it is interesting to examine the budget for high latitudes separately. Although the CTMs do not represent the O_3 depletion events in the Arctic boundary layer, this should have negligible effect on the budget. The same budget analysis as shown above has been made for just the northern high-latitude troposphere: 60°–90°N, surface to 350 hPa, and is shown in Figure 7. The seasonal variation in the ozone mass is somewhat different in the two models, with HANK having a greater amount of ozone from February to May, but less ozone than MOZART by summer. The lower sun angles, lower temperatures, and lack of sources in this region result in a somewhat different balance of terms than seen for the 30°–90°N region (Figure 7b). There is also a greater difference between MOZART and HANK in this region. Both models are dominated by transport until at least March. The larger stratospheric input in HANK (by 5 Tg/mon) is compensated by horizontal export. In MOZART the relatively small stratospheric input is compensated by horizontal input. Net chemical production is near zero for both

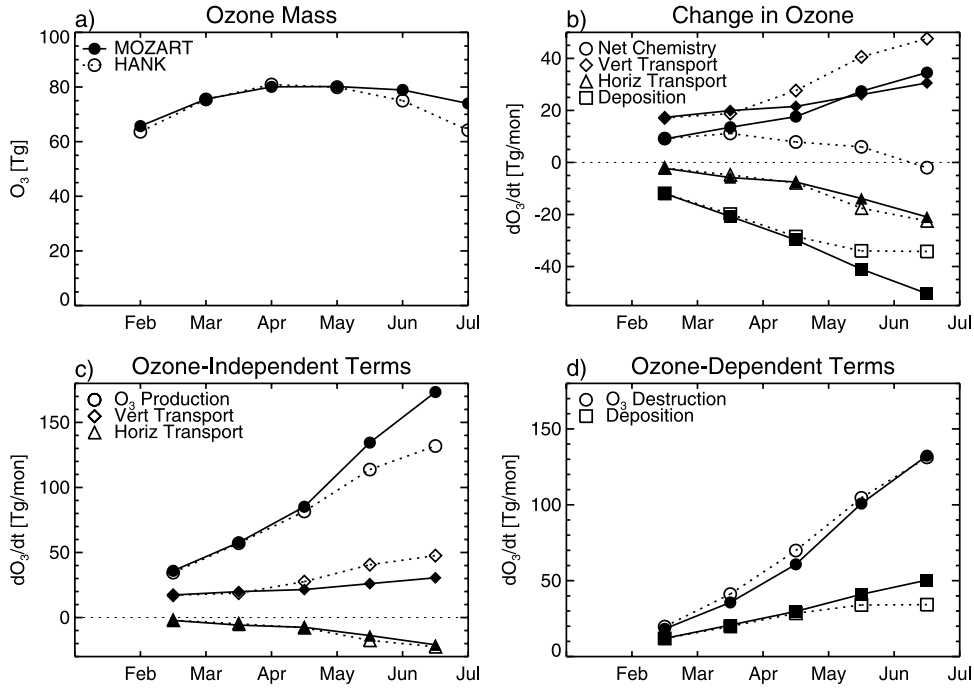

Figure 5. Ozone budget of MOZART (filled symbols) and HANK (open symbols) for the northern middle and high latitudes (30°–90°N, surface to 350 hPa). (a) Total O_3 mass for first day of each month. (b) Monthly rates of change in ozone mass, due to chemistry, horizontal (northward) and vertical (downward) transport and deposition. (c) Contributions to ozone sources: chemical production and net transport. (d) Contributions to ozone sinks: chemical destruction and deposition.

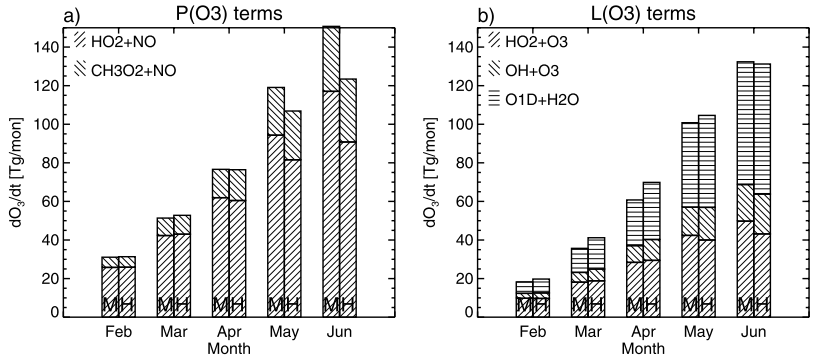

Figure 6. Monthly mean ozone production and loss rate terms for MOZART and HANK zonally integrated over 30°–90°N, surface to 350 hPa.

models until May, at which point MOZART becomes net productive, while HANK is net destructive. Deposition is almost identical in the two models.

[27] In May and June, gross production becomes the dominant term for both models. The chemical loss and deposition terms are quite similar in the two models (Figure 7d), and show a similar increase with season as for the 30°–90°N budget, except that in early spring the increase is proportionally slower. The slightly higher ozone loss rate in May for HANK and significantly higher production rate in June for MOZART, result in the difference in the net chemistry between the two models.

5.4. Ozone Budget for TOPSE Region Versus Zonal Averages

[28] The previous sections have presented zonally averaged ozone budgets of the northern middle and high latitudes. Chemical production and loss as a function of location and altitude are now examined. Figure 8 shows the monthly mean altitude distributions of ozone production and loss. Figure 8a shows the instantaneous production and loss values along the TOPSE flight tracks from steady state calculations constrained by observations of a number of species (including O_3, NO_x, CO, CH_4, peroxides, PAN, HNO_3, NMHCs, and photolysis rates) [*Cantrell et al.*, 2003], MOZART and HANK. The results are averaged over latitudes south and north of 60°N. Both CTMs generally underestimate the calculated production rates at 40–60°N, but match the loss rates well. The steady state calculations show greater production rates at 2–3 km for 40°–60°N, because of the large emissions from Denver at 2 km elevation that are not resolved in the large model grids. The data below 1 km are from samples over North Dakota and Winnipeg, which have much lower emissions than the Denver area. At 60°–90°N the CTMs systematically underestimate the SS rates, but with decreasing bias through spring. Note that the overall values in the higher latitude bin are up to 10 times smaller than the lower latitude bin. The

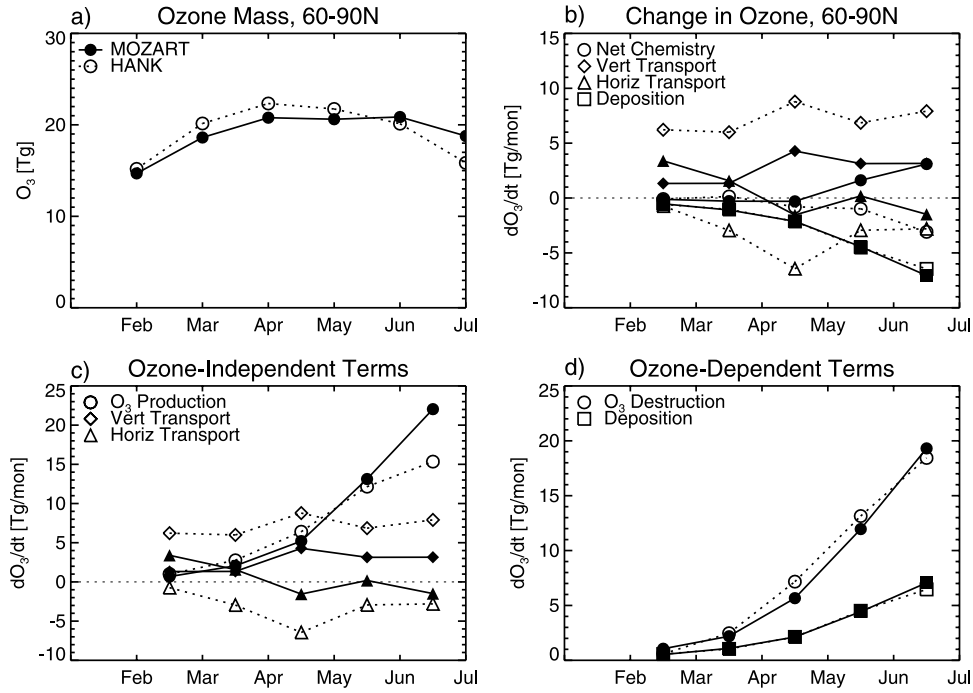

Figure 7. Same as Figure 5, except for 60°–90°N.

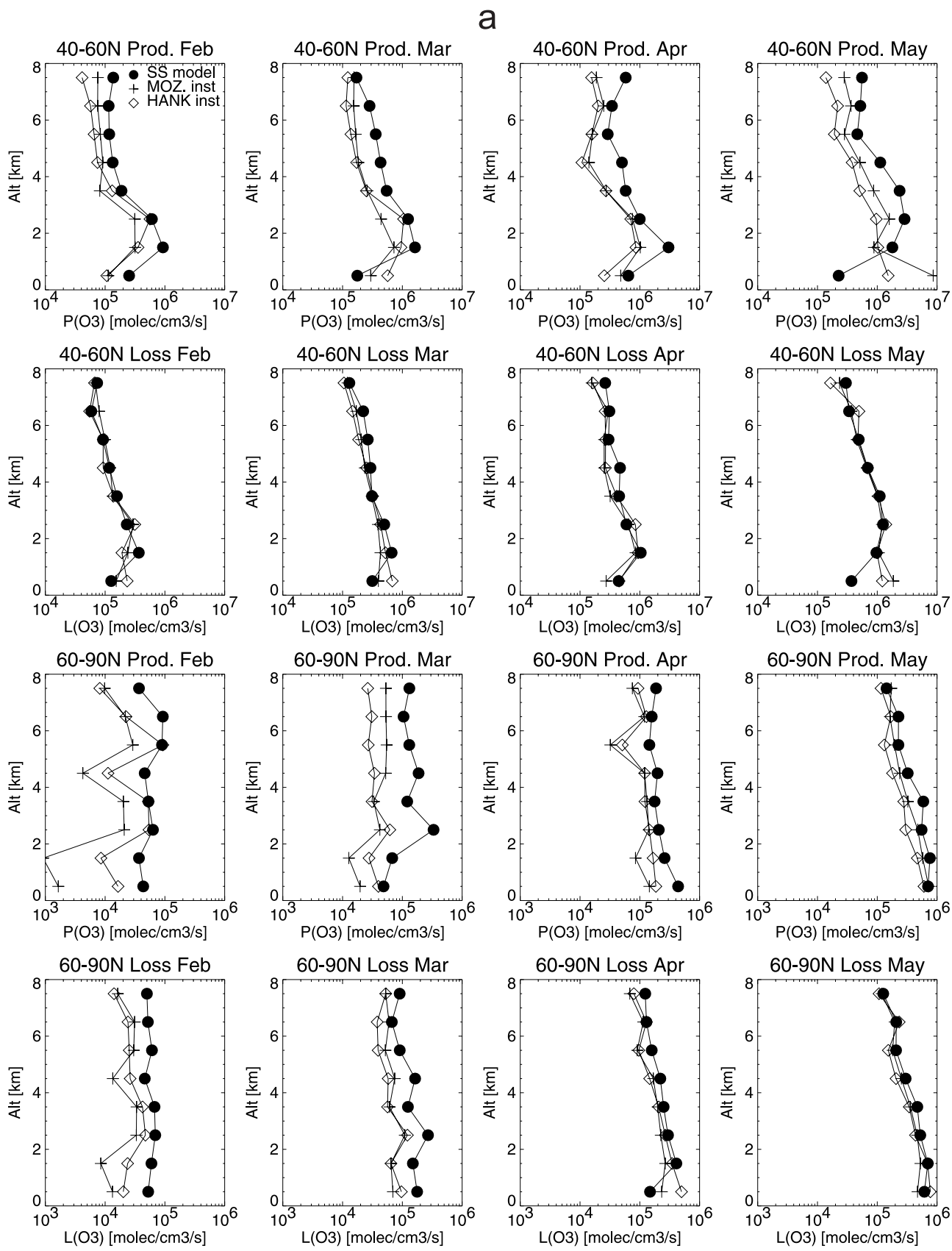

Figure 8. Ozone production and loss as a function of pressure altitude, for monthly means in two latitude bands. (a) Steady state model results [*Cantrell et al.*, 2003] and instantaneous production and loss rates from MOZART and HANK along the flight tracks. (b) Diurnal averages along the flight tracks and zonal averages from MOZART and HANK. Note scale change for latitude bands.

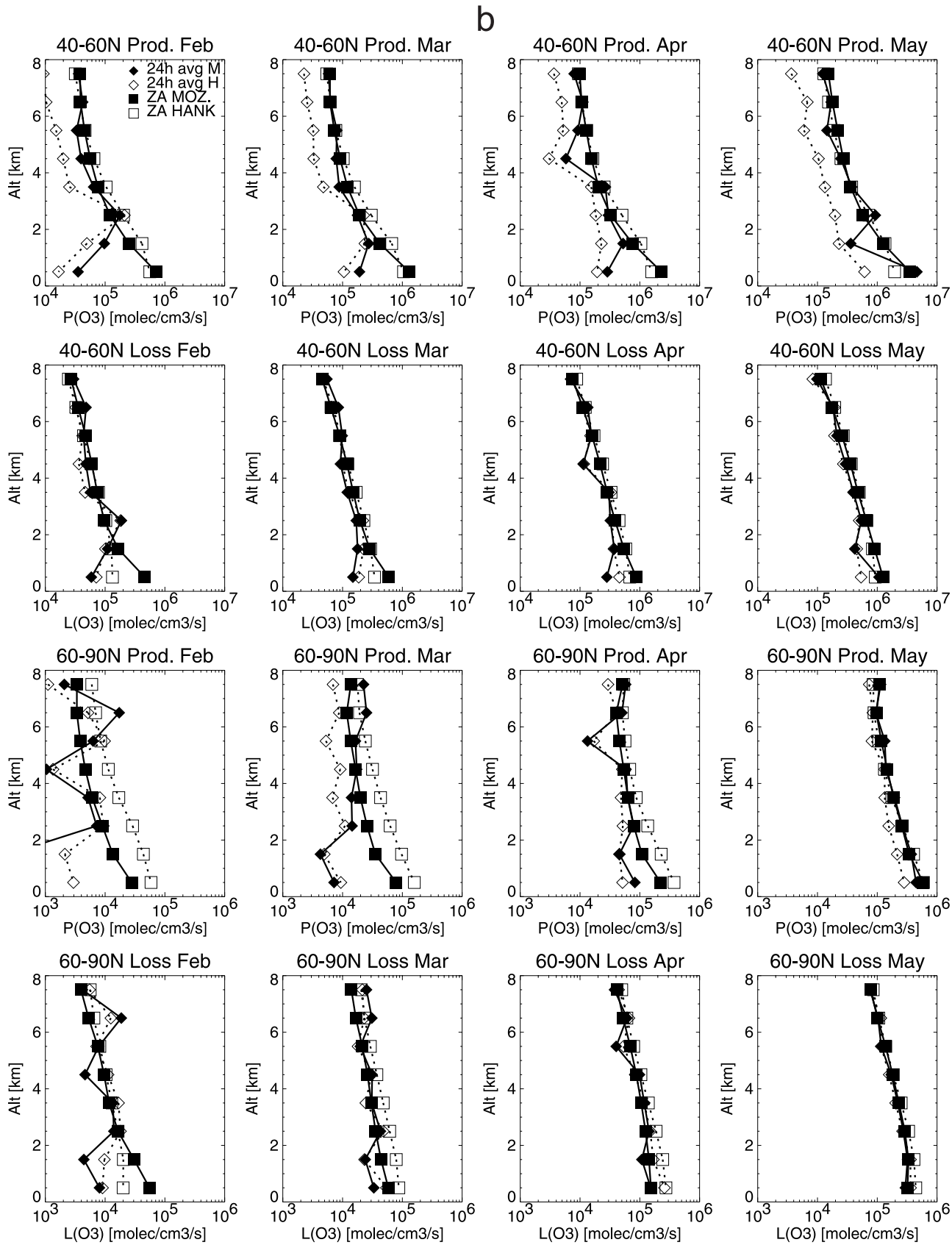

Figure 8. (continued)

Table 4. Production, Loss and Their Difference (P-L) Rates (Tg/mon) From MOZART and HANK, Zonal Monthly Means Integrated Over Surface to 350 hPa for Indicated Latitude Ranges[a]

	MOZART			HANK		
Month	P	L	P-L	P	L	P-L
			30°–40°N			
Feb	29.5	17.5	12.0 (32.8)	25.8	15.1	10.7 (29.2)
March	42.3	27.2	15.0 (41.0)	38.7	28.0	10.7 (29.3)
April	52.3	36.9	15.3 (41.9)	46.7	39.6	7.1 (19.5)
May	71.6	52.5	19.1 (52.2)	59.7	54.1	5.6 (15.3)
June	83.1	59.8	23.3 (63.6)	66.2	61.8	4.4 (12.0)
			40°–60°N			
Feb	15.4	11.1	4.3 (7.4)	16.8	6.9	9.9 (17.2)
March	28.5	18.9	9.6 (16.7)	30.3	16.6	13.6 (23.7)
April	48.5	31.4	17.1 (29.7)	46.1	31.6	14.4 (25.1)
May	80.2	51.4	28.8 (50.1)	62.7	47.8	14.8 (25.8)
June	104.7	68.5	36.2 (62.9)	73.0	61.7	11.3 (19.6)
			60°–90°N			
Feb	0.5	1.0	−0.5 (−1.4)	1.3	0.7	0.6 (1.6)
March	1.6	1.9	−0.2 (−0.7)	3.4	2.9	0.5 (1.4)
April	4.9	5.7	−0.8 (−2.3)	7.7	8.3	−0.6 (−1.7)
May	13.9	12.6	1.3 (3.7)	13.9	14.7	−0.8 (−2.3)
June	23.0	20.0	2.9 (8.4)	17.1	20.0	−3.0 (−8.4)

[a]Net production is also given normalized by area, in parentheses (10^{-14} Tg/mon/m^2). (Areas: 30°–40°N, 3.66×10^{13} m^2; 40°–60°N, 5.75×10^{13} m^2; 60°–90°N, 3.53×10^{13} m^2).

lower modeled O_3 production rates in the CTMs are consistent with the underestimate of NO by the models. Better agreement is seen in the loss rates.

[29] Figure 8b compares the diurnal averages of the model results along the flight tracks with zonal averages from MOZART and HANK. The zonal average shows that the majority of the chemical activity occurs in the boundary layer (0–2 km) at both high and middle latitudes. These zonally averaged low-altitude values are significantly larger than the flight track values, most likely indicating the effect of local emissions not sampled along the flight tracks. The zonally averaged net production (P-L, not shown) is positive for all months at 40°–60°N in the lower 3 km for both models, but near zero in the midtroposphere. However, at the high latitudes, net production occurs only in the lowest 1 km in late spring, and net destruction throughout the rest of the troposphere. The diurnally averaged flight track results show the same structure as the instantaneous results (Figure 8a), but are about half of the magnitude.

[30] Table 4 shows the latitudinal contributions of production and loss from MOZART and HANK to the ozone budget shown in Figure 5. In all three latitude bands the production and loss increase from winter through spring in both models. In February and March the 30°–40°N band contains the largest fraction of the production and loss. The 40°–60°N band has the largest area of the three bands, but shows comparable integrated rates to the lower latitude band in April and May. The high-latitude band (60°–90°N) makes the smallest contribution (<15%) to the total region (i.e., 30°–90°N) for all months, and makes a negligible contribution until the solar flux increases late in the spring. When normalized by area, it is evident that net production at the lower latitudes is most important for this region in late winter and early spring, while in the 40°–60°N band net production is comparable to the lower latitudes for the second half of spring. The lower levels of precursors and sunlight at the high latitudes keep the net production rates low, and at times negative.

[31] In the two lower latitude bands HANK has significantly less production than MOZART in May and June, causing the difference seen in Figure 5. MOZART and HANK show rather different values and trends in net production. At 30°–40°N, MOZART net production doubles from February to June, while HANK decreases by a factor of 1.5. At 40°–60°N, MOZART increases by a factor of 9, but HANK only increases by 50%, peaking in April–May.

5.5. Steady State Ozone

[32] The spring maximum in ozone can be understood in terms of the approach of ozone to its photochemical equilibrium value. To see this we write O_3 at photochemical steady state as:

$$[O_3]_{ss} = ([V] + [H] + [P])/(\tilde{L} + \tilde{D}), \quad (2)$$

where the terms with a tilde represent the respective terms in equation (1) multiplied by ozone, integrated over the volume and divided by the volume integral of ozone, and square brackets indicate integrals over the same volume. In the following analysis these terms are evaluated using output from each of the two models. Calculations by *Klonecki* [1999] suggest that this is a reasonable approximation for ozone production (P) and loss (L). The deposition rate (D) is a function of meteorological parameters which do not depend on O_3. The vertical transport (V) is assumed to be dependent on the ozone in the lowermost stratosphere, but not on tropospheric ozone. The horizontal flux largely depends on horizontal ozone gradients in the troposphere, which we assume remain constant as ozone approaches its steady state concentration.

[33] Substituting equation (2) in (1), the ozone evolution equation can be rewritten in terms of its steady state value:

$$\frac{d[O_3]}{dt} = (\tilde{L} + \tilde{D})([O_3]_{ss} - [O_3]). \quad (3)$$

[34] The timescale to reach equilibrium is simply $(\tilde{L} + \tilde{D})^{-1}$, i.e., it is equal to the steady state ozone concentration divided by its input ($V + H + P$). The relation between ozone and its steady state concentration for MOZART and HANK for each month is shown in Figure 9a for the northern extratropical troposphere (i.e., zonally averaged for latitudes >30 N and pressures >350 hPa). Despite the differences in the ozone budget between the two models, they give a remarkably similar picture of the spring ozone maximum. Ozone is driven up toward large steady state ozone values during the winter and early spring. However, the time constant with which ozone is being driven to these higher values is very slow (shown in Figure 9c) and consequently ozone does not reach the very high equilibrium concentrations. In mid- and late spring, the steady state ozone concentrations decrease to below the actual O_3 values, mainly due to increased chemical loss. The spring ozone maximum occurs when ozone reaches its steady state value. To our knowledge, there have not been other steady state analyses such as this. Other global model analyses have shown positive net ozone production through winter and early spring, without accounting for the effect of

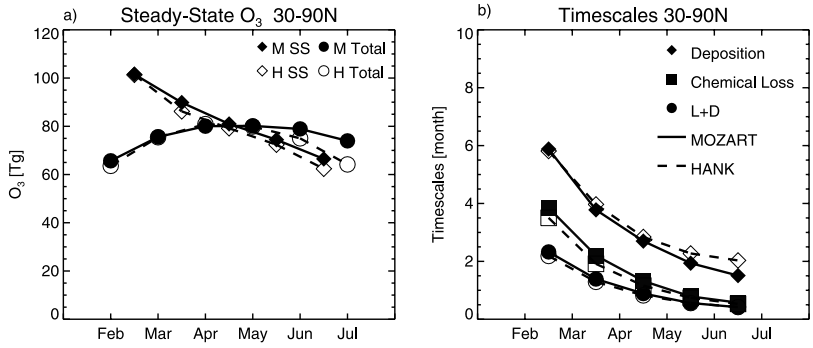

Figure 9. Monthly mean steady state ozone mass and timescales for MOZART and HANK. (a) Ozone mass for 30°–90°N, surface to 350 hPa: calculated steady state O_3 (equation (2)) is plotted at midmonth, with the model-simulated total ozone mass for the first of each month (from Figure 5). (b) Timescales for ozone deposition, chemical loss, and deposition plus loss; 30°–90°N.

vertical flux in the net production [e.g., *Yienger et al.*, 1999; *Wang et al.*, 1998].

5.6. Stratospheric Contribution

[35] There has been considerable debate concerning the tropospheric contribution to the springtime ozone maximum (through in situ ozone production) versus the stratospheric contribution (through the stratospheric flux of ozone). To some extent the ''stratosphere versus troposphere'' debate probably persists due to ambiguities in defining and quantifying the stratospheric ozone flux and the tropospheric ozone production. Moreover, neither of these quantities is directly measurable in the field. This has necessitated using indirect measures of deducing their relative importance [e.g., see *Browell et al.*, 2003], or relying on model studies.

[36] Below we show the sensitivity of tropospheric ozone to the stratospheric ozone flux, and apply two measures of the relative importance of the stratosphere versus the troposphere in explaining the springtime ozone maximum to the model simulations. Each measure gives a quantitatively different answer. We discuss the interpretations of these measures, their assumptions and their limitations. Neither measure quantifies the indirect impact of stratospheric ozone flux on tropospheric ozone production and loss cycles. We do not address this issue here, but it is addressed by *Lamarque et al.* [1999].

5.6.1. Measure 1

[37] This measure simply compares the net stratospheric ozone flux against tropospheric ozone production. From the steady state O_3 definition in equation (2), the influence of the stratosphere can be measured as $V/(V + H + P)$, the fraction of the total ozone input due to the stratospheric flux. Note that this can be interpreted as the stratospheric portion of ozone at steady state.

[38] We do not use the net tropospheric ozone production (i.e., $P - LO_3$) in this comparison (see section 5.1). While the net ozone production is explicitly calculated, the determination of P and L requires additional assumptions. In particular, consistent definitions for P and L depend on the explicit definition of O_x [e.g., *Johnston and Kinnison*, 1998]. Useful definitions for O_x eliminate the fast chemical cycling involved in ozone production, at least to the extent possible. Two different definitions were used in HANK for O_x, one simply including the species O_3, $O(^1D)$ and NO_2; the other including the additional species NO_3, N_2O_5, HNO_4 and HNO_2. The average production and loss rates differ by approximately a factor of two between these schemes (not shown). Differences of this order show the difficulty in quantifying the stratospheric influence.

[39] This comparison uses the net vertical stratospheric flux. The net ozone flux is the small difference between the large respective fluxes in each direction (not shown). *Lamarque and Hess* [1994] showed this to be true even when using potential vorticity as the vertical coordinate. As a thought experiment consider the case where the stratospheric flux of ozone into the troposphere exactly balances the tropospheric flux of ozone into the stratosphere. In this case the effect of stratospheric input is simply to replace ozone molecules produced in the troposphere with those from the stratosphere. In such a case, according to this measure, the stratosphere has no direct influence. This assumption is further discussed below in measure 2.

[40] The global net transport from the stratosphere in MOZART-2 (standard version driven with MACCM3) is estimated to be 343 Tg/year (Horowitz et al., submitted manuscript, 2002). This is just below the range of 475 ± 120 Tg/year determined by *McLinden et al.* [2000], and of other studies (391–1440 Tg/year) [*Prather et al.*, 2001]. Somewhat surprisingly, the vertical ozone flux at 350 hPa (Figure 5) shows a very slow increase in both models in the early spring (February–April) then increasing more rapidly until the simulations end in June. While a number of studies have suggested the highest ozone fluxes occur during spring, *Appenzeller et al.* [1996] shows the mass flux across the tropopause has a relative maximum in midwinter and a stronger maximum in late spring (May–June). The flux across 350 hPa is not the same as the cross-tropopause flux, but it is assumed here to be comparable.

[41] The ratio, $V/(V + H + P)$, determined from the MOZART and HANK budgets given in Figure 5c, is included in Table 5. The fraction determined from the MOZART results decreases steadily from 33% in February to 16% in June. In HANK, however, there is a slight minimum in the stratospheric fraction in February–March, but the fraction is about 30% throughout spring. These numbers should be considered an upper bound, as both models significantly underestimate NO_x and are therefore likely to underestimate in situ ozone production in the

Table 5. Estimates of the Relative Importance of Stratospheric Flux and In Situ Production on Tropospheric Ozone Determined From: Measure 1, the Fraction of Total Ozone Input Due to Stratospheric Flux ($V/(V + H + P)$); Measure 2, the Stratospheric Ozone Tracer (O_3^s/O_3); and a Sensitivity Test of the Effect of a Perturbation in Vertical Flux to Tropospheric Ozone (($\Delta O_3/O_3$)/($\Delta V/V$))[a]

Month	$\frac{V}{V+H+P}$, %	O_3^s/O_3, %	$\frac{\Delta O3/O3}{\Delta V/V}$, %
Feb	33 (34)	56	16
March	27 (26)	49	16
April	21 (27)	43	16
May	17 (29)	36	16
June	16 (30)	31	14

[a]See text for discussion. Results are from MOZART except values in parentheses are from HANK.

ambient low NO_x conditions (e.g., see the steady state model calculations of production in Figure 8a).

5.6.2. Measure 2

[42] A second measure of stratospheric influence uses a tracer of stratospheric ozone which is only destroyed in the troposphere. This has been used in numerous 3-d model calculations [e.g., *Roelofs and Lelieveld*, 1997; *Wang et al.*, 1998]. Table 5 shows the ratio of this stratospheric tracer to tropospheric ozone for MOZART. The results suggest that 56% of tropospheric ozone is of stratospheric origin in February. This fraction drops steadily through spring, to 31% in June. Other studies suggest this ratio is probably on the order of 20–40% [e.g., *Roelofs and Lelieveld*, 1997; *Wang et al.*, 1998]. This latter ratio is consistent with the ratio of vertical transport to the total ozone input in February (from measure 1, Table 5).

[43] This measure of stratospheric influence makes different assumptions with regard to the stratospheric flux of ozone than made in measure 1 above. Therefore one would not expect the conclusions of these two measures to be quantitatively the same. Nor can we offer a judgment on the preferred method. Instead we simply discuss the implicit assumptions made using this measure.

[44] Measure 2 makes the same assumptions as measure 1 with regard to ozone loss: it is explicitly calculated using a set of explicit assumptions. The implicit assumptions with regard to the vertical flux of ozone are somewhat more difficult to ascertain for measure 2. Again, consider the thought experiment where the stratospheric flux of ozone into the troposphere exactly balances the tropospheric flux of ozone into the stratosphere. In this case the concentration of the stratospheric tracer in the troposphere would be nonnegligible, and measure 2 would show considerable stratospheric influence. This is in stark contrast to measure 1. However, measure 2 does not strictly assume the importance of the stratosphere is measured by the downward component of stratospheric ozone flux. There is likely to be some cancellation of the stratospheric tracer transported into and out of the troposphere. The extent of this cancellation is likely to be sensitive to the exact vertical coordinate used to denote the upper boundary of the troposphere. Thus this measure is likely to differ depending on exactly how it is implemented. Indeed, we find that in an experiment with MOZART the tropospheric concentration of the stratospheric tracer is sensitive to exactly how we relax this tracer to stratospheric ozone concentrations above the tropopause.

5.6.3. Sensitivity Test

[45] One measure of the influence of the stratosphere is the sensitivity of tropospheric ozone to an increase in the stratospheric ozone flux. This sensitivity is given by: $\Delta O_3/O_3$ over $\Delta V/V$, where ΔV is the perturbation in the stratospheric flux and ΔO_3 is the tropospheric response. This sensitivity test gives a well defined answer to a well defined question. However, it gives little information concerning the importance of the production of ozone relative to the vertical flux. We have conducted a sensitivity experiment in MOZART by perturbing the stratospheric flux of ozone into the troposphere. We keep the perturbation small ($\Delta V/V \approx 1\%$) so as to remain within a linear regime. In each of the months examined $\Delta O_3/O_3$ over $\Delta V/V$ is on the order of 15% (see Table 5). Thus the troposphere shows relatively small sensitivity to changes in stratospheric ozone flux.

[46] Assumptions about what we mean by the influence of the stratosphere affect our conclusions about how important it is. These assumptions are implicit in the measures given above. The two measures above show a rather small influence of the stratosphere, and the sensitivity test shows a rather small sensitivity to changes in the stratospheric ozone flux. This is not to say that the stratospheric portion of the ozone is not important. It is in fact partly the stratospheric portion which sets the timing of the ozone maximum. *Lamarque et al.* [1999] found that a global model simulation with no stratosphere-troposphere exchange produces a late springtime O_3 maximum in the Northern Hemisphere extratropics. When STE is included the maximum is shifted one month earlier.

6. Discussion

[47] Using two chemical transport models we have studied the ozone budget over the location and time of the TOPSE campaign. The observations from TOPSE have provided an extensive and unique data set with which to evaluate the models. We have shown that the models are generally able to reproduce the observations of ozone and related species. Ozone from the models agrees well with observations from the aircraft and ozonesondes in the upper troposphere, suggesting that the stratosphere-troposphere exchange is reasonable in the models. The models slightly underestimate the in situ aircraft measurements of O_3 below 450 hPa, and generally underestimate NO_x. Reasons for this underestimate are not understood, and may be caused by incorrect parameterization of $N_2O_5 + H_2O$ on aerosols, or the aerosol distribution, or other processes. In some instances there are significant differences in the ability of the two models to reproduce the data. H_2O is overestimated in HANK, while $J(O_3)$ is too low in MOZART. Comparisons with the steady state calculations from the aircraft observations indicate that both MOZART and HANK underestimate the rate of O_3 production. We attribute this to the model shortfall in NO_x (as discussed above).

[48] Differences between HANK and MOZART are indicative of the degree of uncertainty in such analyses. The net chemical production (Figure 5b) is the small difference between the large production and loss rates (Figures 5c

and 5d) and therefore is quite sensitive to relatively small errors in the production and loss terms. For the 30°–90°N zonal volume, the MOZART results indicate increasing net ozone production into May, while HANK suggests the maximum net production occurs in winter and early spring. The difference between these two simulations sensitively depends on both the ozone production and loss rates. While the aircraft measurements suggest water in HANK is somewhat high, we find no systematic discrepancies overall in the photolysis rate of ozone between HANK and the measurements. Thus, even for models with similar chemical mechanisms and emissions, the net production of ozone can depend sensitively on the model formulation and meteorology. These aspects of these simulations will be evaluated more thoroughly in future work.

[49] Although the O_3 mixing ratios and total masses are quite similar in the two models, the balance of chemistry and transport can be significantly different at times. HANK has a larger stratospheric input from April through June. This is partly compensated by less net ozone production due to increased photochemical ozone losses in March and April and decreased ozone production in May and June. Other compensating factors also exist. For example, despite the fact that 2000 was an anomalously low year for Arctic stratospheric ozone, the ozone in the upper troposphere and lower stratosphere in both models agrees with the sonde data. Moreover, while MOZART underestimates the photolysis of ozone, $O(^1D)$ is nearly the same in both models.

[50] Despite the numerous measurements made during TOPSE, it is not possible to conclude whether MOZART or HANK is more correct in the cases where they disagree. In some cases there are not sufficient measurements, or the measurement and modeling uncertainties are large (e.g., OH, HO_2, RO_2). Our limited knowledge of the accuracy of some of the model inputs, such as wind fields and emissions, also introduces uncertainties to these results. The magnitude of stratosphere-troposphere exchange is extremely difficult to evaluate in the models, and critically affects the budget calculations. The precise balance of chemistry and transport depends sensitively on these model details, and therefore remains uncertain.

[51] We have hypothesized that the ozone increase during the spring months can be attributed to the fact that ozone is less than its steady state concentration. The steady state ozone concentration decreases during the spring months as the ozone loss increases. The springtime ozone maximum is reached when ozone equals the steady state ozone concentration. The measures of stratospheric fraction indicate its contribution to the spring maximum is small.

[52] Our simulations complement the work of *Cantrell et al.* [2003] and *Wang et al.* [2003], who show the ozone budget along the flight tracks using steady state and diel box model calculations, respectively. We show that the budgets are similar when extended over the Northern Hemisphere. All of the model results show a strong increase in ozone production and loss rates through spring, with significantly more production at 40°–60°N, than at higher latitudes. The production of ozone is dominated by the reaction HO_2 + NO, and ozone loss is primarily due to $HO_2 + O_3$ and $O(^1D) + H_2O$, with the contribution from $O(^1D) + H_2O$ increasing most rapidly through spring. Our conclusions are also qualitatively similar to *Yienger et al.* [1999], showing that both production and loss increase significantly through spring. However, their simulation produces 60 pptv of NO_x in March for 60°–70°N in the midtroposphere, whereas the TOPSE observations are 10–30 pptv.

7. Conclusions

[53] The ozone budget during the period of the TOPSE campaign has been analyzed using results from MOZART and HANK. Although the models produce differing results in some aspects, they show the same overall conclusions. These results indicate that the Northern Hemisphere spring ozone maximum is driven by an increase in photochemistry through the spring months. The ozone production is between a factor of two (in February) and a factor of five (in May) times larger than the transport from the stratosphere (30°–90°N). We compare the gross production, not the net production, against the transport, as ozone loss operates on stratospheric as well as tropospheric ozone. This conclusion holds in both models using different meteorological analyses with different vertical resolutions. Analyses of a model experiment where vertical flux is perturbed and of a stratospheric ozone tracer in MOZART result in qualitatively similar conclusions. Given the good correlations between ozone in the upper troposphere and the measurements, it seems likely that tropospheric ozone production dominates over transport during the spring months.

[54] **Acknowledgments.** We thank S. Madronich and F. Flocke for helpful comments and discussions. The comments of three reviewers helped improve the clarity of the paper. Ozonesonde data were obtained from the World Ozone and Ultraviolet Data Centre, http://www.msc-smc.ec.gc.ca/woudc/index.html. LE was partially supported by NASA IA L-9301. The National Center for Atmospheric Research is operated by the University Corporation for Atmospheric Research under the sponsorship of the National Science Foundation.

References

Abbatt, J. P. D., Interaction of HNO_3 with water-ice surfaces at temperatures of the free troposphere, *Geophys. Res. Lett.*, *24*, 1479–1482, 1997.

Appenzeller, C., J. R. Holton, and K. H. Rosenlof, Seasonal variation of mass transport across the tropopause, *J. Geophys. Res.*, *101*, 15,071–15,078, 1996.

Atlas, E. L., B. A. Ridley, and C. Cantrell, The Tropospheric Ozone Production about the Spring Equinox (TOPSE) Experiment: Introduction, *J. Geophys. Res.*, *108*(D4), 8353, doi:10.1029/2002JD003172, 2003.

Barth, M. C., P. J. Rasch, J. T. Kiehl, C. M. Benkovitz, and S. E. Schwartz, Sulfur chemistry in the National Center for Atmospheric Research Community Climate Model: Description, evaluation, features, and sensitivity to aqueous chemistry, *J. Geophys. Res.*, *105*, 1387–1416, 2000.

Brasseur, G. P., D. A. Hauglustaine, S. Walters, P. J. Rasch, J.-F. Müller, C. Granier, and X.-X. Tie, MOZART: A global chemical transport model for ozone and related chemical tracers, part 1: Model description, *J. Geophys. Res.*, *103*, 28,265–28,289, 1998.

Brasseur, G. P., J. J. Orlando, and G. S. Tyndall, *Atmospheric Chemistry and Global Change*, Oxford Univ. Press, New York, 1999.

Browell, E. V., et al., Ozone, aerosol, potential vorticity, and trace gas trends observed at high-latitudes over North America from February to May 2000, *J. Geophys. Res.*, *108*(D4), 8369, doi:10.1029/2001JD001390, 2003.

Cantrell, C. A., et al., Steady state free radical budgets and ozone photochemistry during TOPSE, *J. Geophys. Res.*, *108*(D4), 8361, doi:10.1029/2002JD002198, 2003.

European Centre for Medium-Range Weather Forecasting (ECMWF), The description of the ECMWF/WCRP Level III-A Global Atmospheric Data Archive, Reading, UK, 1995.

Giorgi, F., and W. L. Chameides, The rainout parameterization in a photochemical model, *J. Geophys. Res.*, *90*, 7872–7880, 1985.

Grell, G. A., J. Dudhia, and D. R. Stauffer, A description of the fifth generation Penn State/NCAR Mesoscale Model (MM5), *NCAR/TN-398+IA*, Natl. Cent. for Atmos. Res., Boulder, Colo., 116 pp., 1993.

Hallquist, M., D. J. Stewart, J. Baker, and R. A. Cox, Hydrolysis of N_2O_5 on submicron sulfuric acid aerosols, *J. Phys. Chem. A*, *104*, 3984–3990, 2000.

Hauglustaine, D. A., G. P. Brasseur, S. Walters, P. J. Rasch, J.-F. Müller, L. K. Emmons, and M. A. Carroll, MOZART: A global chemical transport model for ozone and related chemical tracers, part 2: Model results and evaluation, *J. Geophys. Res.*, *103*, 28,291–28,335, 1998.

Hess, P. G., Model and measurement analysis of springtime transport and chemistry of the Pacific basin, *J. Geophys. Res.*, *106*, 12,689–12,717, 2001.

Hess, P. G., S. Flocke, J.-F. Lamarque, M. C. Barth, and S. Madronich, Episodic modeling of the chemical structure of the troposphere as revealed during the spring MLOPEX 2 intensive, *J. Geophys. Res.*, *105*, 26,809–26,840, 2000.

Holton, J. R., P. H. Haynes, M. E. McIntyre, A. R. Douglas, R. B. Rood, and L. Pfister, Stratosphere-troposphere exchange, *Rev. Geophys*, *33*, 403–439, 1995.

Jöckel, P., R. von Kuhlmann, M. Lawrence, B. Steil, C. Brenninkmeijer, P. Crutzen, P. Rasch, and B. Eaton, On a fundamental problem in implementing flux-form advection schemes for tracer transport in 3-dimensional general circulation and chemical tracer models, *Q. J. R. Meteorol. Soc.*, *127*, 1035–1052, 2001.

Johnston, H., and D. Kinnison, Methane photooxidation in the atmosphere: Contrast between two methods of analysis, *J. Geophys. Res.*, *103*, 21,967–21,984, 1998.

Kiehl, J. T., T. L. Schneider, P. J. Rasch, and M. C. Barth, *J. Geophys. Res.*, *105*, 1441–1457, 2000.

Klonecki, A., Model study of the tropospheric chemistry of ozone, Ph.D. thesis, Princeton Univ., Princeton, N. J., 1999.

Klonecki, A., P. Hess, L. Emmons, L. Smith, J. Orlando, and D. Blake, Seasonal changes in the transport of pollutants into the Arctic troposphere-model study, *J. Geophys. Res.*, *108*(D4), 8367, doi:10.1029/2002JD002199, 2003.

Lamarque, J.-F., and P. G. Hess, Cross-tropopause mass exchange and potential vorticity budget in a simulated tropopause folding, *J. Atmos. Sci.*, *51*, 2246–2269, 1994.

Lamarque, J.-F., and P. G. Hess, Model analysis of the temporal and geographical origin of the CO distribution during the TOPSE campaign, *J. Geophys. Res.*, *108*(D4), 8354, doi:10.1029/2002JD002077, 2003.

Lamarque, J.-F., P. G. Hess, and X. X. Tie, Three-dimensional model study of the influence of stratosphere-troposphere exchange and its distribution on tropospheric chemistry, *J. Geophys. Res.*, *104*, 26,363–26,372, 1999.

Logan, J., An analysis of ozonesonde data for the troposphere: Recommendations for testing 3-D models and development of a gridded climatology for tropospheric ozone, *J. Geophys. Res.*, *104*, 16,115–16,149, 1999.

Mauldin, R. L., III, C. A. Cantrell, M. A. Zondlo, E. Kosciuch, B. A. Ridley, R. Weber, and F. E. Eisele, Measurements of OH, H2SO4, and MSA during Tropospheric Ozone Production About the Spring Equinox (TOPSE), *J. Geophys. Res.*, *108*(D4), 8366, doi:10.1029/2002JD002295, 2003.

McLinden, C. A., S. C. Olsen, B. Hannegan, O. Wild, M. J. Prather, and J. Sundet, Stratospheric ozone in 3-D models: A simple chemistry and the cross-tropopause flux, *J. Geophys. Res.*, *105*, 14,653–14,665, 2000.

Müller, J.-F., Geographical distribution and seasonal variation of surface emissions and deposition velocities of atmospheric trace gases, *J. Geophys. Res.*, *97*, 3787–3804, 1992.

Müller, J.-F., and G. Brasseur, IMAGES: A three-dimensional chemical transport model of the global troposphere, *J. Geophys. Res.*, *100*, 16,445–16,490, 1995.

Olivier, J. G. J., A. F. Bouwman, C. W. M. van der Maas, J. J. M. Berdowski, C. Veldt, J. P. J. Bloos, A. J. H. Visschedijk, P. Y. J. Zandveld, and J. L. Haverlag, Description of EDGAR version 2.0: A set of global emission inventories of greenhouse gases and ozone-depleting substances for all anthropogenic and most natural sources on a per country basis and on a 1 × 1 degree grid, *RIVM Rep. 771060 002*, *TNO-MEP Rep. R96/119*, Natl. Inst. of Public Health and the Environ., Bilthoven, Netherlands, 1996.

Oltmans, S., and H. Levy II, Surface ozone measurements from a global network, *Atmos. Environ.*, *23*, 9–24, 1994.

Penkett, S. A., and K. A. Brice, The spring maximum in photochemical oxidants in the Northern Hemisphere, *Nature*, *319*, 655–657, 1986.

Pickering, K. E., Y. Wang, W.-K. Tao, C. Price, and J.-F. Muller, Vertical distributions of lightning NOx for use in regional and global chemical transport models, *J. Geophys. Res.*, *103*, 31,203–31,216, 1998.

Prather, M., et al., Atmospheric chemistry and greenhouse gases, in *Climate Change 2001: The Scientific Basis*, *Contribution of Working Group I to the Third Assessment Report of the Intergovernmental Panel on Climate Change*, edited by J. T. Houghton et al., 881 pp., Cambridge Univ. Press, New York, 2001.

Price, C., and D. Rind, A simple lightning parameterization for calculating global lightning distributions, *J. Geophys. Res.*, *97*, 9919–9933, 1992.

Price, C., J. Penner, and M. Prather, NO_x from lightning, 1, Global distribution based on lightning physics, *J. Geophys. Res.*, *102*, 5929–5941, 1997.

Randel, W. J., F. Wu, J. M. Russell III, A. Roche, and J. Waters, Seasonal cycles and QBO variations in stratospheric CH4 and H2O observed in UARS HALOE data., *J. Atmos. Sci.*, *55*, 163–185, 1998.

Rasch, P. J., M. C. Barth, J. T. Kiehl, S. E. Schwartz, and C. M. Benkovitz, A description of the global sulfur cycle and its controlling processes in the National Center for Atmospheric Research Community Climate Model, version 3, *J. Geophys. Res.*, *105*, 1367–1386, 2000.

Richard, E. C., et al., Severe chemical ozone loss inside the Arctic polar vortex during winter 1999–2000 inferred from in situ airborne measurements, *Geophys. Res. Lett.*, *28*, 2197–2200, 2001.

Ridley, B. A., et al., Ozone depletion events observed in the high latitude surface layer during the TOPSE aircraft program, *J. Geophys. Res.*, *108*(D4), 8356, doi:10.1029/2001JD001507, 2003.

Roelofs, G.-J., and J. Lelieveld, Model study of the influence of cross-tropopause O_3 transports on tropospheric O_3 levels, *Tellus, Ser. B*, *49*, 38–55, 1997.

Shetter, R. E., and M. Müller, Photolysis frequency measurements on the NASA DC-8 during the PEM-Tropics Mission using actinic flux spectroradiometry: Instrument description and results, *J. Geophys. Res.*, *104*, 5647–5661, 1999.

Shetter, R. E., L. Cinquini, B. L. Lefer, S. R. Hall, and S. Madronich, Comparison of airborne measured and calculated spectral actinic flux and derived photolysis frequencies during the PEM Tropics B mission, *J. Geophys. Res.*, *107*, 8234, doi:10.1029/2001JD001320, 2002 [printed *108*(D2), 2003].

Sinnhuber, B.-M., et al., Large loss of total ozone during the Arctic winter of 1999/2000, *Geophys. Res. Lett.*, *27*, 3473–3476, 2000.

Simmonds, P. G., S. Seuring, G. Nickless, and R. G. Derwent, Segregation and interpolation of ozone and carbon monoxide measurements by air mass origin at the TOR station Mace Head, Ireland from 1987–1995, *J. Atmos. Chem.*, *28*, 45–59, 1997.

Thompson, A. M., M. A. Huntley, and R. W. Stewart, Perturbations to tropospheric oxidants, 1985–2035, 1: Calculations of ozone and OH in chemically coherent regions, *J. Geophys. Res.*, *95*, 9829–9844, 1990.

Tie, X., G. Brasseur, L. Emmons, L. Horowitz, and D. Kinnison, Effects of aerosols on tropospheric oxidants: A global model study, *J. Geophys. Res.*, *106*, 22,931–22,964, 2001.

Tie, X., et al., Effects of sulfate aerosol on tropospheric NOx and ozone budgets: Model simulations and TOPSE evidence, *J. Geophys. Res.*, *108*(D4), 8364, doi:10.1029/2001JD001508, 2003.

Wang, Y., D. J. Jacob, and J. A. Logan, Global simulation of tropospheric O_3 -NO_x -hydrocarbon chemistry, 3, Origin of tropospheric ozone and effects of nonmethane hydrocarbons, *J. Geophys. Res.*, *103*, 10,757–10,767, 1998.

Wang, Y., et al., Springtime photochemistry at northern mid and high latitudes, *J. Geophys. Res.*, *108*(D4), 8358, doi:10.1029/2002JD002227, 2003.

Wesely, M. L., Parameterization of surface resistances to gaseous dry deposition in regional-scale numerical models, *Atmos. Environ.*, *23*, 1293–1304, 1989.

Yienger, J. J., A. A. Klonecki, H. Levy II, W. J. Moxim, and G.R. Carmichael, An evaluation of chemistry's role in the winter-spring ozone maximum found in the northern midlatitude free troposphere, *J. Geophys. Res.*, *104*, 3655–3667, 1999.

E. Atlas, C. Cantrell, F. Eisele, L. K. Emmons, P. Hess, D. Kinnison, J.-F. Lamarque, R. L. Mauldin, B. Ridley, R. Shetter, and X. Tie, Atmospheric Chemistry Division, National Center for Atmospheric Research, P.O. Box 3000, Boulder, CO 80307, USA. (atlas@ucar.edu; cantrell@ucar.edu; eisele@ucar.edu; emmons@ucar.edu; hess@ucar.edu; mauldin@ucar.edu; dkin@ucar.edu; lamar@ucar.edu; ridley@ucar.edu; shetter@ucar.edu; xxtie@ucar.edu)

G. Brasseur, Max Planck Institute for Meteorology, Bundesstrasse 55, D-20146 Hamburg, Germany. (brasseur@dkrz.de)

E. Browell, Atmospheric Sciences Research, NASA Langley Research Center, Mail Stop-401A, Hampton, VA 23681-0001, USA. (e.v.browell@larc.nasa.gov)

L. Horowitz, GFDL/NOAA, Princeton University, P.O. Box 308, Princeton, NJ 08542-0308, USA. (lwh@gfdl.noaa.gov)

A. Klonecki, NOVELTIS, Parc Technologique du Canal, 2, Avenue de l'Europe, F-31520 Ramonville-Saint-Agne, France. (klonecki@lsce.saclay.cea.fr)

J. Merrill, Graduate School of Oceanography, Center for Atmospheric Chemistry Studies, University of Rhode Island, Narragansett, RI 02882-1197, USA. (jmerrill@boreas.gso.uri.edu)